Chapter 2
Introduction to Optical Characterization of Materials

Julio A.N.T. Soares

2.1 Introduction

The use of light to probe the physical and chemical properties of matter is a concept more natural than most of us realize. We have been doing this since our early years with our vision. For example, we can estimate how hot is an incandescent object by the color of light it emits, see the variation on the thickness of a soap film by the different colors of light it transmits, or the relative concentration of some solutions by the amount of light it absorbs. There are many more examples of the use of light to characterize the world around us, which we perform in our daily routines. The use of specialized instrumentation to extend the range, acuity, sensitivity, and precision of our vision or to quantitatively use photons of light to determine materials properties is what we call optical characterization.

There are many different characterization techniques that use photons with energies in the range of the electromagnetic spectrum which we call light (with energies between 1.2 meV and 124 eV). In this chapter our intention is to give a brief introduction to a few of the most popular examples of these techniques, with an emphasis on its applicability, usefulness, and limitations. We will talk about techniques that can be used complementarily and discuss some of the hurdles which are commonly encountered when using them in practical, real world application examples, offering suggestions on how to avoid them whenever possible.

Optical characterization techniques are usually non-destructive, fast, and of simple implementation, most requiring very little sample preparation. These techniques explore the change on intensity, energy, phase, direction, or polarization of the light wave after interaction with the object being studied. Many of them can be performed at room temperature and atmosphere, dispensing the use of complex vacuum chambers. That, allied to the fact that the optical properties of a material

J.A.N.T. Soares (✉)
University of Illinois at Urbana-Champaign
e-mail: soares@illinois.edu

M. Sardela (ed.), *Practical Materials Characterization*,
DOI 10.1007/978-1-4614-9281-8_2, © Springer Science+Business Media New York 2014

depend on its structural, morphological, electronic and physical properties, make them very powerful characterization techniques.

Optical properties of materials have played a major role in the advancement of science and our current understanding of the universe. A few significant examples are:

- The study of the blackbody radiation, which lead to the formulation of quantum mechanics by Max Plank.
- The discovery and study of the photoelectric effect, which provided evidence of the dual nature of light.
- The study of the optical emission from atoms and molecules, which provided evidence of their quantized electron energy levels. The chemical element helium was discovered from the observation of the emission spectrum of the Sun.

Much of the technology we use daily is based on optics and photonics, thus on light and its interaction with matter. CD, DVD, and Blue Ray players and recorders, barcode scanners, digital cameras, liquid crystal displays, fiber optics communication, lasers, household and street lightning, car lights, paints, dyes, inks, laser printers are a few of many more examples. In each of these applications, many years of research and development were spent. A significant portion of that was optical characterization.

2.2 About Light

What is light? This has been a question that intrigued humans for many centuries. It is essential to our daily lives, and the way we see the world around us is through its interaction with light. In short, light is the electromagnetic radiation with energies between 1.2 meV and 124 eV. It displays a dual nature, i.e. it behaves as particles in some instances and as waves in other. The model for its particle behavior is the photon, a quantum particle, with no mass and no charge that interacts with other particles (electrons, atoms, etc.) electromagnetically. Its energy and wavelength are related by the Planck's constant and the speed of light in vacuum, which is a fundamental constant: $E = hc/\lambda$.

Light, as waves, diffracts, refracts, interferes, and its propagation through space and energy transport can be described in terms of waves motion. Light waves carry energy without carrying mass at a speed that is independent of its intensity. In this model it is described as coupled oscillating magnetic and electric fields.

Light is characterized by its frequency, amplitude (number of photons), direction and speed. Its speed is always c in vacuum, but slower in other media. In glass [1], for example its speed is $^{2}/_{3}$c, in water [2], $^{3}/_{4}$c, and in air [2] it is 0.9997c. The rate of reduction of the speed of light (v) in a material is called the refraction index of that material (n):

$$n = \frac{c}{v} \tag{2.1}$$

The frequency of the light (and thus the energy of the photons) is a characteristic of its source, and it does not change independent of the media the light is traveling through, which means that its wavelength shortens when it slows down in a medium with a higher refraction index. In spectroscopy, when we plot the data against the photon wavelength, we are referring to its wavelength in vacuum. Common units used to plot spectroscopic data are:

Name	Symbol	Relation to λ	Unit
Wavenumber	ν	$^{1}/_{\lambda}$	cm^{-1}
Wavelength	λ	1	μm, nm, Å
Energy	E	$^{hc}/_{\lambda}$	eV
Frequency	ν	$^{c}/_{\lambda}$	Hz

Fundamental constants [3]: $h = 4.13566751(20) \times 10^{-15} eV.s$; $c = 299,792,458\, m/s$

2.2.1 Polarization

We say that a light beam is polarized when the electric fields of all the waves composing that beam oscillate in the same direction. If the direction of its polarization doesn't change with time, we say that the beam is linearly polarized. If it does, we call it elliptically polarized. A particular case of elliptical polarization is the circular polarization, where the direction of the beam's electric field changes, but its amplitude remains constant. To better understand this classification, we can describe the oscillating electric field in terms of its components in two perpendicular directions s and p. In Fig. 2.1 the different polarization states are illustrated according to the s–p representation. If we consider the difference in phase δ between the two polarization components, when $\delta = n\pi$, where n is a natural number, the beam is linearly polarized. If $\delta = (2n + 1)\pi/2$ it is circularly polarized, and elliptically polarized otherwise. When the electric fields of all the waves composing that beam oscillate without a preferred direction, we call that beam unpolarized. If most, but not all electric fields oscillate in a given direction, the beam is termed partially polarized.

Light polarization has many uses in our everyday lives, and chances are that you use it every single day. Liquid crystal displays use polarizers and liquids whose molecules tend to align themselves in relation to each other, the so called liquid crystals. These displays are assembled in a way that the molecules orientation inside each pixel of the display causes a change of the polarization direction of light passing through it. Applying strong enough electric fields to the liquid reorients its molecules, and changes its effect on the polarization of light, allowing the particular pixel to either transmit (bright pixel) or block (dark pixel) light. These displays are widely used on electronic calculators, computer monitors, digital watches, television sets, car dashboards, and many other electronic devices. Another popular application of polarized light are polarizing sunglasses, which

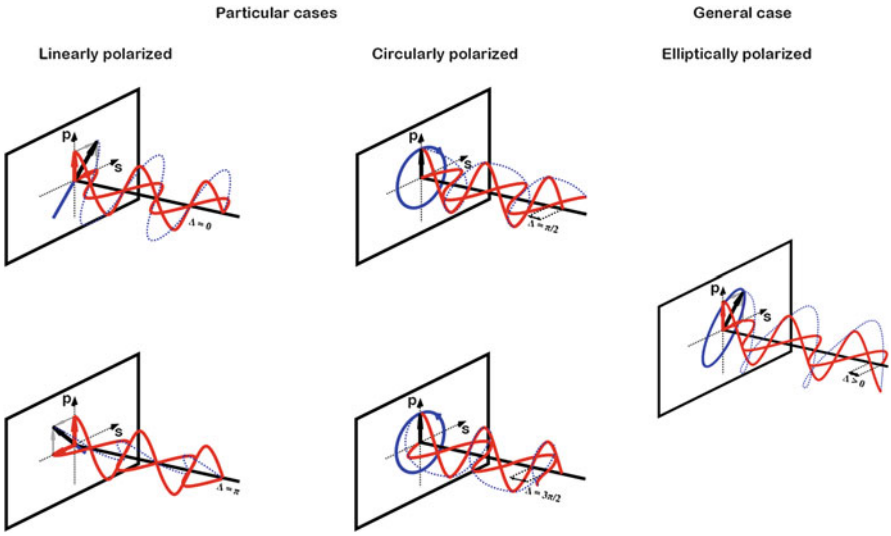

Fig. 2.1 Polarization states of light for particular values of the phase difference Δ between the p and s polarization components

block horizontally linearly polarized light, thus blocking most light reflected by horizontal surfaces, like wet roads, and water bodies' surfaces. Through them we also only see about half of the intensity of the unpolarized light that would otherwise reach our eyes, reducing the brightness of a bright day to a more comfortable level. Other uses of polarized light include three dimensional movies and TVs, photographic filters, optical microscopes, some equipment for stress analysis on plastics, and many others.

2.2.2 Light-Matter Interaction: The Basics

When light interacts with matter, it affects, with its oscillating electromagnetic field, the charges in the material, exchanging energy with that material. In case of dielectrics, the response of the material to an applied electric field is a polarization of its charges. The degree of this polarization depends on the strength of the field and the properties of the material's constituting molecules, and can be quantified by a complex quantity called electric susceptibility, χ. In optics more useful quantities are the complex index of refraction $\tilde{n}$ and the complex dielectric function ε, which are related to χ by [4]:

$$n = n + ik; \chi = \chi' + i\chi'' \tag{2.2}$$

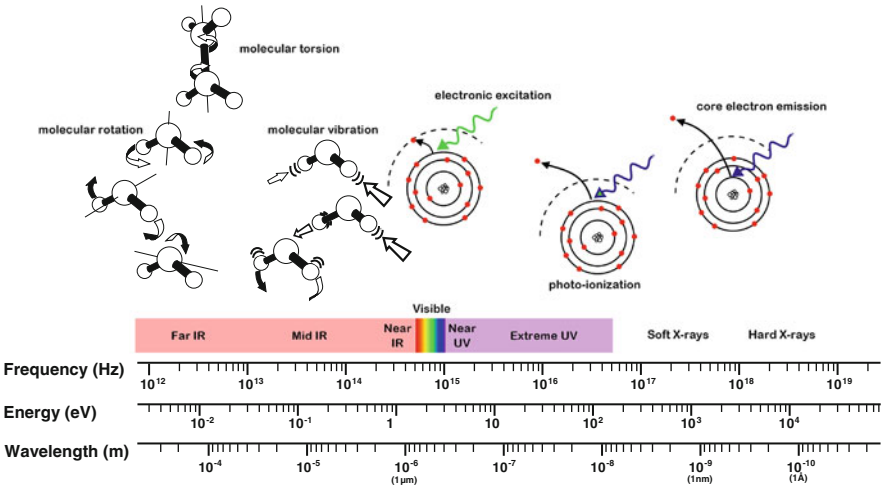

Fig. 2.2 Interaction between light and matter showing the approximate energies of fundamental excitations

$$\varepsilon = \varepsilon_0(1 + \chi) \tag{2.3}$$

$$n^2 + k^2 = 1 + \chi' \tag{2.4}$$

$$2nk = \chi'' \tag{2.5}$$

n and k are also called the index of refraction and coefficient of extinction of the material, and collectively known as the optical constants of the material. By knowing the optical constants of a material, it is possible to mathematically describe and predict its interaction with light.

From a macroscopic point of view, when light impinges on matter, it can be scattered (elastically or inelastically), absorbed, or transmitted. This interaction depends on physical, chemical, and structural properties of the matter, as well as intensity and energy of the photons. Depending on the energy of the photons, different excitations are generated in the matter. Photons on the UV and visible region of the spectrum, for example, are more likely to interact with the electrons of the outer shells promoting them to more energetic levels and/or creating excitons, while infrared photons are more likely to interact with lattice and molecular vibrations and rotations, creating phonons, see Fig. 2.2. Thus, by choosing the appropriate photon energy for our experiments, we can tailor them to investigate different properties of the material. Table 2.1 shows some of these excitations, with a brief description of what they are and a few examples of optical characterization techniques that make use of them.

Table 2.1 Material excitations which can be created by photons with examples of characterization techniques involving such excitations

Excitation	Description	Characteristics	Characterization techniques
Phonon	Collective lattice vibration	Neutral	Raman, IR, photoluminescence
Exciton	Describes the bound state of an electron-hole pair due their mutual Coulomb attraction	Neutral, obey Bose statistics, can bind with impurities, defects and other excitons	Photoluminescence [5], modulation reflectance [6], and transmission
Plasmon	Collective motion of a charge carriers gas with respect to a oppositely charged rigid background	Neutral	UV-VIS, IR, Raman (surface enhanced-SE, tip enhanced-TE) [7]
Polaron	Describes the coupling of electrons or holes and longitudinal phonons	Can bind with other polarons of the same or opposite charge carrier	Absorption [8]
Polariton	Describes the coupling between excitons and phonons		Raman (SE, TE) [9]

2.2.2.1 Absorption

- Absorption, absorbance, absorptance, and coefficient of absorption:

Absorption is the property of the material of transferring energy from the photons to its atoms and molecules. The ratio of the energy transferred to the matter from the incident light to the total incident energy is called absorptance (A), which can be expressed in terms of the reflection (R) and transmission (T) as

$$A = 1 - T - R \tag{2.6}$$

The absorbance (Abs) is another way to measure how much energy is transferred by the incident light to the illuminated object. It is often called the optical density of the object, when interpreted as the attenuation of the incident light by the object. Its relation to the transmission or reflection is given by

$$Abs = -\log_{10}(T) \text{ or } Abs = -\log_{10}(R) \tag{2.7}$$

assuming either R or T being zero for transparent or highly reflective samples respectively.

The coefficient of absorption is the rate at which the light is absorbed when traveling through the material, given by

$$a = \frac{Abs}{\ell} = -\frac{\log_{10}(T)}{\ell}, \tag{2.8}$$

where ℓ is the length of the path the light traveled through the material. Some prefer to give the absorption coefficient using natural logarithms, in which case it is denoted by α, and related to a by $\alpha = a \ln 10$. a can be expressed as a function of the imaginary part of the complex index of refraction k and the wavelength of the incident light λ by

$$a = -\frac{4\pi k}{\lambda} \tag{2.9}$$

2.2.2.2 Light Scattering

- **Elastic scattering**: **Mie and Rayleigh scattering**

The elastic scattering of light is responsible for the color of the blue sky, as well as for the yellow, red and orange tones of the sunrise and sunset. Lord Rayleigh was the first to establish a quantitative theory for the elastic scattering of light by particles whose diameter d, is small compared to the wavelength of the light ($d << \lambda$). He calculated the intensity of light scattered by the dipole induced by the light on those particles with a volume v to be [10]:

$$I = I_0 \frac{9\pi^2 v^2}{2R^2\lambda^4} \left(\frac{m^2 - 1}{m^2 + 2}\right)^2 \left(1 + \cos^2\theta\right) \tag{2.10}$$

where R is the distance to the particle and m is the relative index of refraction of the particle to the surrounding medium. That means that light with shorter wavelength is scattered much more efficiently, thus why we see the sky blue during the day. Larger particles scatter the light without a strong dependency on wavelength, thus the color of clouds being white. Rayleigh extended his theory to particles of all sizes and shapes, as long as the particle's index of refraction is comparable to unity. In 1908, G. Mie published the theory of the light scattering for an isotropic absorbing sphere of arbitrary size. His theory was more general than Rayleigh's because it includes absorbing bodies and Rayleigh's theory is a special case of Mie's. For that reason, the scattering of light by larger particles (1/3 of λ or larger) is generally called Mie scattering, while Rayleigh scattering is used for the scattering of small particles.

- **Inelastic scattering**: **Raman and Brillouin scattering**

As we mentioned above, photons incident on a molecule can also excite normal modes of vibration of that molecule, or phonons in a solid. Likewise, it can be scattered by phonons in the material and gain the energy corresponding to those phonons. This inelastic scattering is known as Raman scattering, when optical phonons are involved, or Brillouin scattering when acoustic modes are responsible for the scattering. When the photons emerging from the interaction have a lower

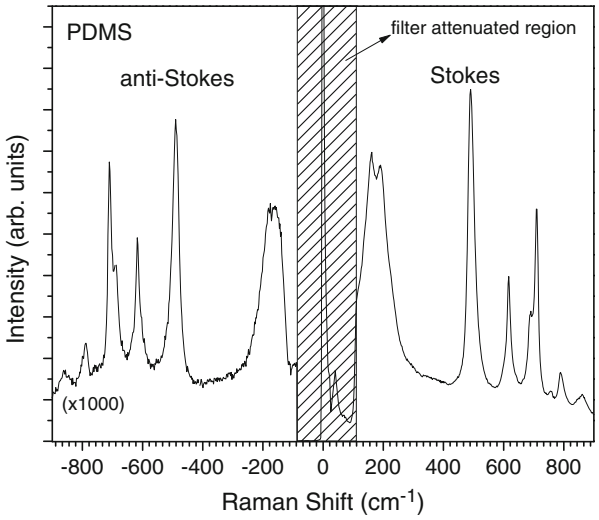

Fig. 2.3 Raman spectrum of a polydimethylsiloxane (PDMS) sample showing the peaks due to anti-Stokes (negative Raman shifts) and Stokes (positive Raman shifts) scattering. The anti-Stokes side of the spectrum has been multiplied by a factor of 1,000 times so it can be seen clearly. The section shadowed is the region of the spectrum which was heavily attenuated by filters, in order to reduce the Rayleigh scattering into the detector

energy than that of the incident photons, we call the interaction Stokes scattering, and term it anti-Stokes scattering otherwise. Figure 2.3 shows the Raman spectrum for a PDMS sample where we can see the peaks related to the Stokes and anti-Stokes Raman scattering. In principle, photons of almost any energy larger than the energy associated to the vibration modes involved can be inelastically scattered. When photons with energies close to that of electronic transitions are used, they can promote resonant scattering.

Since the allowed modes of vibration of a solid or molecule are intimately linked to its structure and chemical composition, inelastic light scattering can be efficiently used as a structural characterization method or as a substance detection and identification tool. Below we will review the Raman scattering and its use as an optical characterization technique in more detail.

2.3 Spectrophotometry (UV-VIS-NIR)

One of the most basic methods to investigate the properties of materials through their interaction with light, also the most natural to us, is to measure how much light is reflected, transmitted or absorbed by that material. As seen above, a material absorbs light when the incident photons create atomic or charge movements in the material. If we measure that absorption as a function of photon energy, we can get

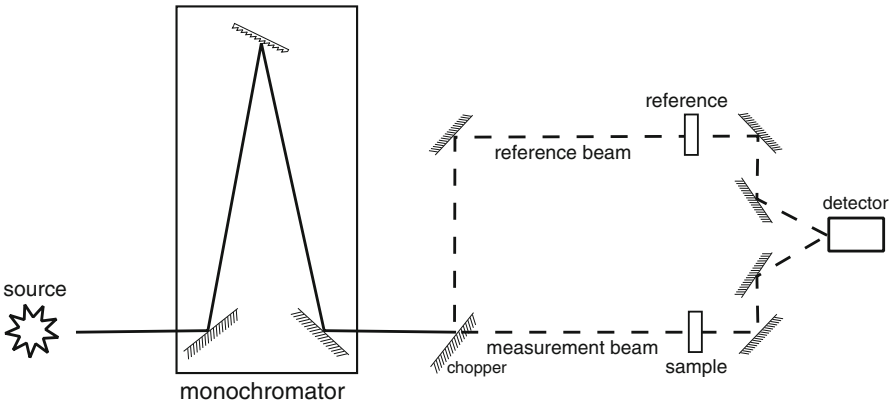

Fig. 2.4 Schematic diagram of a dual beam spectrophotometer operating in transmittance mode

an insight into its electronic and atomic structure. Note that morphology, stress, temperature, contact with other materials, etc. all may affect the materials phonons and electrons transitions and will modify the materials light absorption in many cases. While this is useful, allowing us to know more about the material's properties through the measurement of its absorption spectrum, all these variables must be controlled or monitored when performing the measurements.

Spectrophotometry is one of the most popular modalities of spectroscopies that measure the intensity of transmitted and reflected light. The typical spectral range covered by high-end commercial spans from the near ultra-violet ($\lambda \sim 200$ nm) to the near infra-red ($\lambda \sim 3$ μm). This is the reason many use the term UV-VIS to designate spectrophotometry (the technique), or the spectrophotometer (the instrument).

2.3.1 Instrumentation

There is a wide variety of spectrophotometers in the market, from cheaper single beam models with limited spectral range and measurement capabilities to expensive double beam models featuring multiple light sources and detectors, capable of a wider spectral range and supporting a more diverse set of accessories for a variety of experiments and different types of samples. The most commonly used higher end instruments consist, typically, of a couple light sources, a diffraction grating based monochromator, a sample chamber and one or more detectors. Shown in Fig. 2.4 is the schematic diagram of a simple dual beam spectrophotometer.

Several accessories are available for the higher end spectrophotometers, which enable performing different modalities of measurement on different types of samples, as for example, solid films, liquid solutions, powders, etc. Some of the modalities commonly available are transmittance, diffuse transmittance, diffuse and specular reflectance, and variable angle specular reflectance. Instruments

equipped with two beams allow for the measurement of a reference sample simultaneously with the test sample. Even if no reference sample is used, the reference beam is useful to compensate for possible slow fluctuations of the source intensity or conditions of the detectors that could affect their response.

2.3.2 Transmittance

This is the simplest modality of experiment one can perform with a spectrophotometer and virtually all spectrophotometers can perform transmittance measurements. It consists in measuring how much of a known incident light power (P_0) shining on a sample passes through it, as a function of the light wavelength. It can be expressed as a percentage by

$$T = \frac{P_T}{P_0} \times 100 \tag{2.11}$$

where P_T is the power of the light that made through the sample and T its transmittance.

Light sources do not emit equal intensities of light on all wavelengths, detector response is a function of wavelength, mirrors, windows, gratings, and other optical components in the optical path of the spectrophotometer have efficiencies that vary with photon energy. Therefore, we need to know how all these factors will affect the values read on the detector. We call these contributions to the spectrum not originated from the sample, baseline. Besides the contribution to the spectrum due to the baseline, another source of error on the determination of the absolute transmission is the non-zero response of the detector under dark conditions, the dark current.

To quantify the system baseline, we measure a known sample. To measure the dark current of the detectors, we block the light path by using an opaque sample. These quantities may vary slowly with usage of the instrument, so the best approach is to determine them at the time of each measurement. If our sample is a bulk film, we collect the baseline by doing the measurement without any sample. If our sample has a substrate or a solvent, we do the baseline measurement using a clean piece of substrate or the pure solvent.

After measuring the spectrum from a sample, we subtract the dark current of the detectors (D), then divide the raw spectrum obtained (T_0) by the baseline (B), also corrected for the dark current, to determine the contribution due solely to the sample, the absolute transmittance (T).

$$T = \frac{T_0 - D}{B - D} \tag{2.12}$$

This method compensates for the spectral inhomogeneities of the spectrophotometer components and for contributions from substrates or solvents. It doesn't

compensate for fluctuations on the source intensity or other systematic errors. Some instruments are equipped with two beam paths, a sample beam and a reference beam. The intensities reported by the instrument are, in this case, the ratio between those two beams, measured almost simultaneously. Thus, all the light powers measured of the sample beam are divided by the powers measured of the reference beam:

$$T = \frac{T_0 - D}{B - D} = \frac{{}^{P_S}/_{P_R} - {}^{D_S}/_{D_R}}{{}^{B_S}/_{B_R} - {}^{D_S}/_{D_R}}, \tag{2.13}$$

where the quantities measured of the sample beam path are denoted by the S subscript, and the ones measured of the reference beam by the R subscript.

Since it is not possible to measure two different beam intensities simultaneously on the same single channel detector, the simplest solution is to use an optical element to divert the same beam through two different paths (measurement and reference) alternately, so the detector receives light from either path at alternating moments in time. Each data point in the spectrum will be an average of several of these pulses.

2.3.2.1 Data Acquisition Strategies

Ideally, using the reference beam would make measuring the baseline unnecessary. In practice, due to differences in the optical elements efficiencies and alignment between the two paths the baseline correction is usually still necessary for accurate measurements. The main advantage of the dual beam spectrophotometer is to compensate for short term (seconds to minutes) variations on the light sources intensities and the efficiency of the optical components common to both beams. Most variations in this time scale are due to light source intensities and detector efficiency changes due to temperature variation.

To perform the baseline correction, a reference sample (substrate or solvent) is not needed in the reference beam path. This beam path can remain clear, and the procedure for the measurements is the same as with a single beam spectrophotometer. We may choose to have a reference standard placed in the reference beam, but that beam must be kept the same to acquire the baseline, the dark current, and all the spectra which will be corrected using that baseline. It is important to notice that if we decide to place a reference standard in the reference beam path, an identical reference standard needs to be placed in the sample beam path to measure the baseline. The reference beam should never be blocked.

If we are measuring pure liquids and want to compensate for the transmittance of the container, we should not use the empty container to measure the baseline. Most liquids will have a better refraction index match to the walls of the container than air. Thus, if we use the empty container to measure, we will have an increased portion of the light reflected from those walls, causing a reduction of the absolute value of the transmittance for the baseline, and a corresponding increment on the

transmittances corrected using that baseline. The best method to correct for the transmittance of the container is to measure the baseline with this container filled with a liquid with a refraction index as close as possible to the liquid we want to measure, which has no absorption in the spectral range of the measurement. To check if our reference liquid has no absorption in the desired range, we can simply compare the spectrum of the empty container to that of the reference liquid. If the spectra are identical but for a relatively small constant shift toward larger transmittances for the filled container, the reference liquid is transparent.

2.3.3 Specular Reflectance

Another common use of spectrophotometers is to measure reflectance. The operation of the system for these measurements is very similar to that of the transmittance, except that the beam paths are modified so the light that reaches the detector is the light reflected by the sample. There are two main modalities of reflectance measurements, the diffuse reflectance, where light reflected by the sample in all directions is collected (paper-like reflection); and specular reflectance, where only the light that is reflected by the sample at an angle identical to that of the angle of incidence is collected (mirror-like reflectance).

There are several accessories designed to collect the specular reflectance of samples. A schematic representation of some of the most popular of these accessories is shown in Fig. 2.5.

For this modality of measurements, when collecting the dark current we take the sample out interrupting the beam path by the lack of a reflecting element and for collecting the baseline, we use a known reflectance standard mirror. No standard mirror is perfect, so to calculate the absolute specular reflection of a sample, we need to take the true reflectance curve for the standard mirror used to acquire the baseline into account. For that reason, these accessories are called relative specular reflectance accessories.

Another class of accessories are the absolute specular reflectance accessories (ASRA), like the VW configuration ASRA depicted in Fig. 2.5. For this class of accessories, the optical path and all optical elements are exactly the same for measuring the baseline or the sample, except for the presence of the sample in the beam path. Thus there is no need to correct for the less than perfect reflectance of the reference standard mirror. A disadvantage of this setup is that the sample must be relatively large, to allow for the double bounce of the light on its surface. We also need to be careful when we interpret the spectra obtained with this accessory, since because of the double bounce, we are actually measuring the square of the sample reflectance. This configuration is less indicated for low reflectance samples, since the intensity on the detector falls proportionally to the square of the reflectance.

Another popular ASRA is the VN configuration. In this configuration, the beam only reflects once at the sample surface, but more moving parts are necessary, and the accuracy is critically dependent on alignment and beam and detector homogeneity,

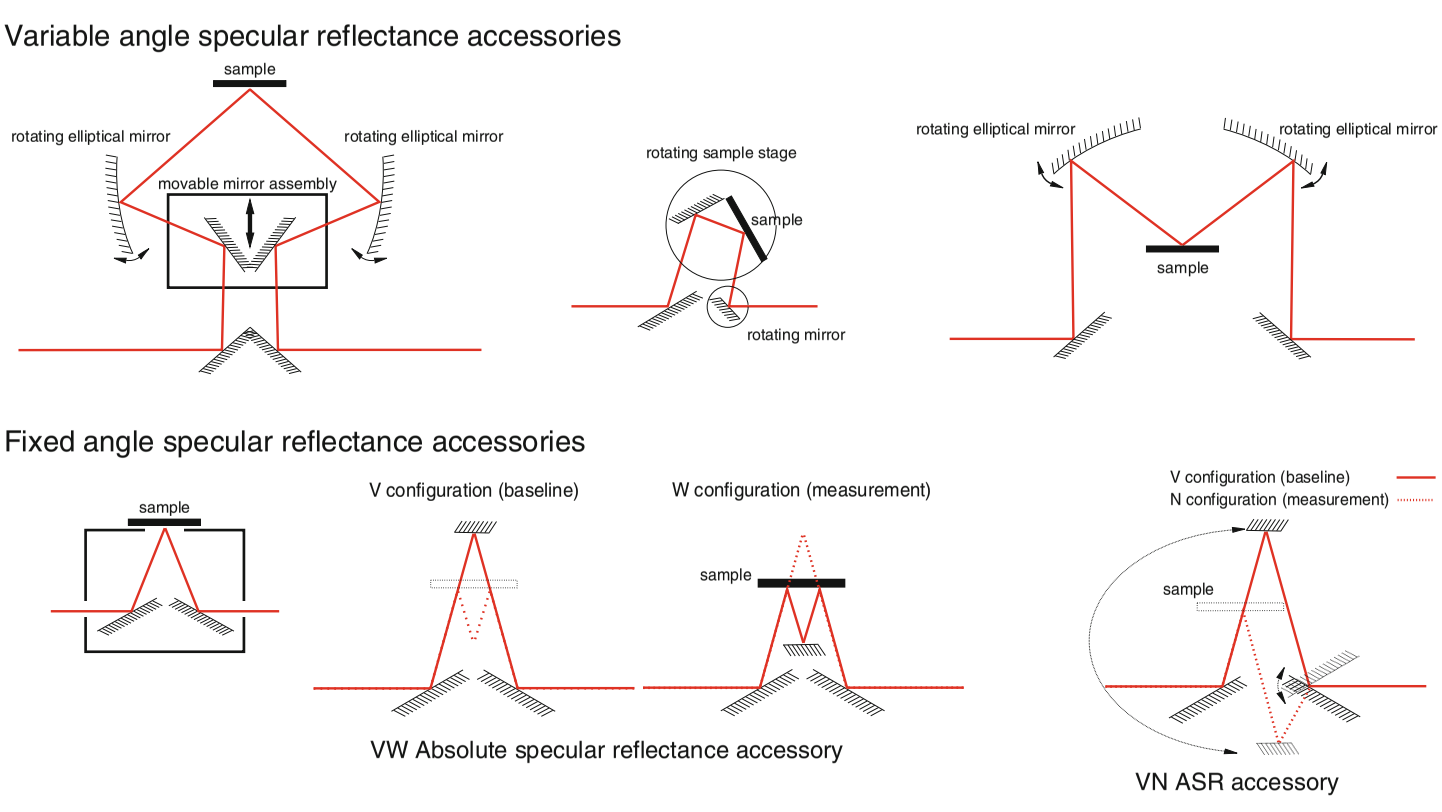

Fig. 2.5 Schematic representation of the beam paths of some popular specular reflectance accessories

since the output beam is reversed between the two configurations. More recently, an automated variable angle ASRA is commercially available. Its design includes a beam path compensator, to adjust for differences in the beam path between sample measurement and baseline collection geometries, a rotating mirror, and a movable detector assembly. All movable parts are controlled by computer, to simplify operation and minimize alignment issues. It is nonetheless a more complex and expensive accessory than the VN and VW ASRA, but also much more flexible than those.

2.3.3.1 Data Acquisition Strategies

When measuring reflectance of films on a substrate, specially transparent or semi-transparent films, it is important to think carefully about how to compensate for the substrate contributions.

The baseline for reflectance must be acquired with the standard mirror designed for this purpose, without any other sample in the beams. One might be tempted to use the substrate to collect the dark current, to account for light which passes through the film and is reflected by the substrate, passing again through the film and reaching the detector. The problem with that approach, though, is that at the spectral regions in which the film is non-transparent, we would be subtracting the contribution from the substrate from a spectrum that does not contain it. Even for the regions were the film is partially transparent, we would be neglecting the double transmission through the film when correcting for the substrate contribution. Thus, the best approach is to not use the substrate at all when collecting the baseline and the dark current. If we want to separate the contribution from the substrate, we must measure the reflectance from the clean substrate, and from the sample with the film separately. Then, we can qualitatively tell the substrate contributions from the film contributions to the final spectrum. We can also calculate the reflectance spectrum due solely to the film if we know the optical constants and thickness for the film and the optical constants for the substrate or iteratively fit these parameters to the experimental data. For a careful analysis of the subject, see [11] and [12].

2.3.4 Diffuse Reflectance

Specular reflectance is indicated when measuring highly polished surfaces. Reflection from rougher surfaces is generally scattered in many directions, not always strongly related to the angle of incidence of the light, as is the case for specular reflection. This is the case of powder samples, most ceramics, paper, nanostructured surfaces, etc. To collect the reflected light from such surfaces, it is necessary to use a specially designed mirror or integrating spheres. The reflectance of the sample is then compared with a standard with a known diffuse reflectance. This modality of measurement is also useful to measure reflective surfaces that distort the incident beam, like curved mirrors.

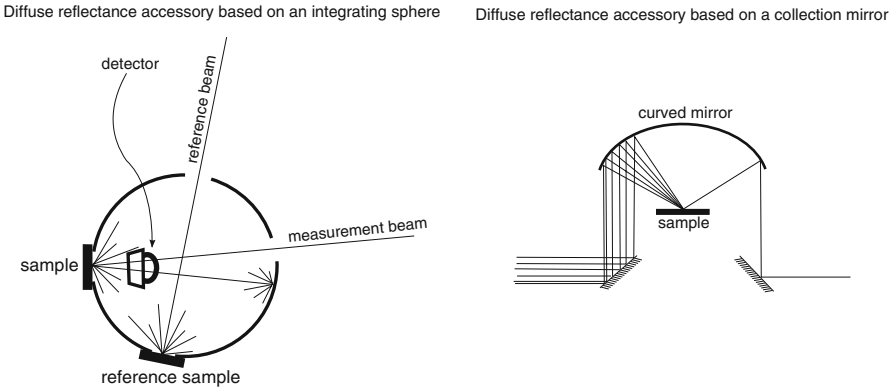

Fig. 2.6 Schematic diagram of diffuse reflectance accessories

Most diffuse reflectance accessories (DRA) are capable of discarding the specular component of the light reflected from the sample, in case we wish to measure only the diffuse component of the reflectance of a sample.

Figure 2.6 shows the schematic representation of two DRA, one based on an integrating sphere and another based on a specially designed curved mirror. Integrating spheres are internally coated with special materials, which have a very high (>90 %) non-specular (to decrease geometrical effects) spectrally flat reflectance over the wavelength range it is intended to be used. Although their very reflective coating, integrating spheres have an inherently high loss, making the measurement of samples with very low reflectance challenging to measure accurately.

DRA based on mirrors cannot collect the diffuse reflectance in all directions, making them a less accurate instrument for samples with an anisotropic diffuse reflection.

Diffuse reflected light undergoes repeated transmission through the sample, thus the low absorption bands are emphasized in comparison with the transmission spectrum of the same sample. To compensate, the Kubelka-Munk function has to be applied to the diffuse reflectance spectrum for comparison to the transmission spectrum or to make a quantitative analysis to determine concentration.

In 1931, Kubelka and Munk [13] proposed a system of differential equations assuming a simplified model for propagation of light in a dull (no specular reflection) painted layer parallel to a plane support. They assumed this layer isotropic and homogeneous, except for optical heterogeneities small in comparison to the thickness of the layer. They also considered that only two diffuse fluxes need to be accounted for: one in the direction of incidence and another in the opposite direction and they ignored geometrical variations of light distribution through the painted layer. Finally, they assumed absorption (K) and scattering (s) coefficients to be independent of the thickness of the layer and ignored polarization and spontaneous emission. Kubelka and Munk solved this system of equations and obtained the reflectance value associated to a given wavelength in the case of an infinite (R_∞)

or finite (R) painted layer, in terms of the absorption and scattering coefficients and the reflectance of the support (R_0) [14]. For a sufficiently thick layer (opaque) the solution Kubelka and Munk derived becomes

$$\frac{K}{s} = \frac{(1 - R_\infty)^2}{2R_\infty}. \tag{2.14}$$

Their formula and its applicability are still a subject of intense discussion [14–16].

The Kubelka-Munk equation is frequently used by industries that fabricate dyes and paints such as textiles, paper, and coatings [16]. For these applications, the scattering (S) of light by a paint or dye is assumed to depend on the properties of the substrate (solvent, binder, and additives), while the absorption (K) of light depend on the properties of the pigment. The Kubelka-Munk equation is roughly linear with respect to pigment concentration:

$$\frac{K}{s} = \eta C \tag{2.15}$$

where η is a constant.

2.3.5 *Diffuse Transmittance*

Diffuse transmission may also be collected using integrating sphere based DRA. To perform this measurement, we place the sample on the entrance aperture designed for the sample beam and cover the sample aperture with the standard high reflectivity sample. The baseline and dark current are collected exactly like the non-diffuse transmittance and analysis is the same as diffuse reflectance.

2.3.6 *Absorbance*

Most reports in the published literature calculate the absorbance of a sample from either its transmittance or the reflectance spectra, assuming that all the light that is not transmitted (if we are calculating it from the transmittance spectrum) is absorbed. The absorbance calculated in this fashion is effectively the attenuation that sample exerts on the light, i.e. its optical density, when transmitting or reflecting the light, see Sect. 2.2.2.1 above.

Measuring low absorbances accurately by taking the R and T spectra of a sample can be very challenging. This is due to the fact that small errors in any of the two measurements may be greater than the absorbance itself. To work around this difficulty, some instrument manufacturers offer a center mount integrating sphere accessory. With this accessory we can take the diffuse R and T spectra simultaneously, using the exact same sampling and geometry, so it is easier to calculate the absorbance

of the sample. A caution that must be taken when using this accessory is that not only the spot where the light hits the sample is being measured, but the non-directly illuminated parts of the sample also are contributing to the total absorbance.

2.3.6.1 Beer-Lambert Law

One of the most common uses of spectrophotometry is to quantify the concentration of solutions from their absorbance spectra. The Beer-Lambert [17] law states that the absorbance of a solution is linearly proportional to its concentration c, and the path length ℓ of the light in the solution. The proportionality coefficient is the molar absorptivity K. Thus,

$$Abs = \mathrm{K}\ell \cdot \mathrm{c} = a\ell \tag{2.16}$$

where a is the absorption coefficient.

Some conditions may lead to a non-linearity of the absorbance with concentration:

- Highly concentrated solutions may present deviations in molar absorptivity due to electrostatic interactions between molecules in close proximity, cause large changes in the index of refraction of the solution, and changes in the chemical equilibrium.
- Particulates in the sample may cause light scattering, reducing the transmittance.
- Samples that fluoresce or phosphoresce, and stray light and/or non-monochromatic radiation reaching the detector will cause errors in the determination of the transmittance.

2.3.7 Applications

Among the numerous other applications of spectrophotometry, some of the most relevant examples are:

– Determination of the optical spectra of filters and other optical elements.
– Determination of solution concentration from the absorbance spectrum.
– Determination and observation of reaction kinetics.
– Color measurement, for paints, dyes, coatings.
– Food and food color analysis.
– Multicomponent analysis of pharmaceuticals.
– Band gap determination [18].
– Electronic structure study.

Table 2.2 gives a list of a few general uses of spectrophotometry on the characterization of different types of materials, listing the most commonly used accessories for that application, and a few observations about the measurement procedure.

Table 2.2 Some common applications of spectrophotometry with usual accessories needed for the specific application

Type of sample	Application	Accessories needed	Observations
Liquids (pure)	Transmittance spectra	Transmission	Baseline with a spectrally flat liquid with similar n should be collected for better accuracy
	Color analysis		
Liquids (solutions)	Transmittance spectra	Transmission	Baseline with solvent must be collected
	Color analysis		
	Concentration		From application of Beer-Lambert law
	Reaction kinetics		May require special flow cells
	Scattered transmission spectra	Diffuse reflection accessory (DRA)	DRA to be used in transmission mode
Solid (powders)	Diffuse reflectance spectra	DRA with powder samples holder	
	Color analysis		
Solid (bulk)	Transmittance spectra	Transmission	
	Specular reflectance spectra	Specular reflectance accessory (SRA)	
	Diffuse reflectance spectra	DRA	
	Diffuse transmission spectra		
	Thickness	All	From interference fringes for semi-transparent or transparent samples, with two parallel and flat surfaces
	Band gap and electronic structure		Calculated from optical spectra
	Color analysis		
Solid (thin film on substrate)	Transmittance spectra	Transmission	Requires transparent substrate
	Specular reflectance spectra	SRA	
	Diffuse reflectance spectra	DRA	
	Diffuse transmission spectra		Requires transparent substrate
	Thickness	All (type of substrate may limit which accessory may be used)	From interference fringes for semi-transparent or transparent films, with two parallel and flat surfaces
	Band gap and electronic structure		Calculated from optical spectra
	Color analysis		

This table does not intend to be exhaustive of all uses of spectrophotometry, but to give a few examples of its most common applications for each type of sample

2.3.7.1 Application Example: Thin Films Thickness Determination

When light is transmitted or reflected by a system containing two or more parallel interfaces separating two regions with different index of refraction, beams with a different number of bounces at the interfaces will emerge with a phase difference Δ that is dependent on the wavelength of the light and the path difference between the two beams. The path difference is determined by the thickness of the regions with different indexes of refraction, the value of those indexes, and the angle of incidence of the light. These beams will interfere when emerging from the system, causing the transmission (or reflection) so that the total intensity of light will vary, being maximum when Δ is a multiple of 2π (constructive interference) and minimum when Δ is an odd multiple of π (destructive interference). For light with an angle of incidence θ, wavelength λ transmitting through (reflecting from) a thin free standing film of thickness d and index of refraction n, the interference maxima (minima) will occur when:

$$\lambda m = {}^{m}/_{\nu} = 2nd \ \sin\theta, \tag{2.17}$$

where m is an integer number and ν the wavenumber of the light. If the film is on a substrate of a higher index of refraction, the above equation will give the condition for the fringes minima for transmission and maxima for reflection. If the substrate has a lower index of refraction, the conditions are the same as for the free standing films. This happens due to the change in phase for light reflected from the interface between a lower index and a higher index material. Fortunately, the equation above can be written in a form that allow the calculation of film thickness or index of refraction disregarding the question if the fringes are in a reflectance or transmission spectrum or if there is a substrate or not [19].

Here we will illustrate a simpler case, often encountered when measuring the transmission or reflection of thin films at normal incidence. In this case, $\sin\theta$ is 1, and plotting the fringes position in wavenumbers against m/2n will give us a straight line whose slope is equal to the thickness of the film responsible for creating the fringes. In Fig. 2.7 we see the transmission spectrum for two thin films on a thick substrate. Clear interference fringes can be seen from the thinner adhesive layer, while the fringes for the thicker polyester film appear on the longer wavelength part of the spectrum, with a much smaller amplitude. These higher frequency fringes are frequently missed and confused with noise by inexperienced spectroscopists. The inset on the figure gives a clearer view of the higher frequency fringes. On the plots on the right, the procedure for the determination of the films thicknesses is shown. For this example we considered the refraction indices of both films to be constant over the measured range of wavelengths (1.66 for polyester and 1.5 for the adhesive). The fact that the plots on the right show a very good linearity between m/2n and wavenumber, means that this is a reasonable approximation.

For this example we obtain thicknesses of 2.8 μm for the adhesive layer and 51 μm for the thin polyester film. This is a very practical and simple method for determining the thickness and index of refraction of thin films, but require that we

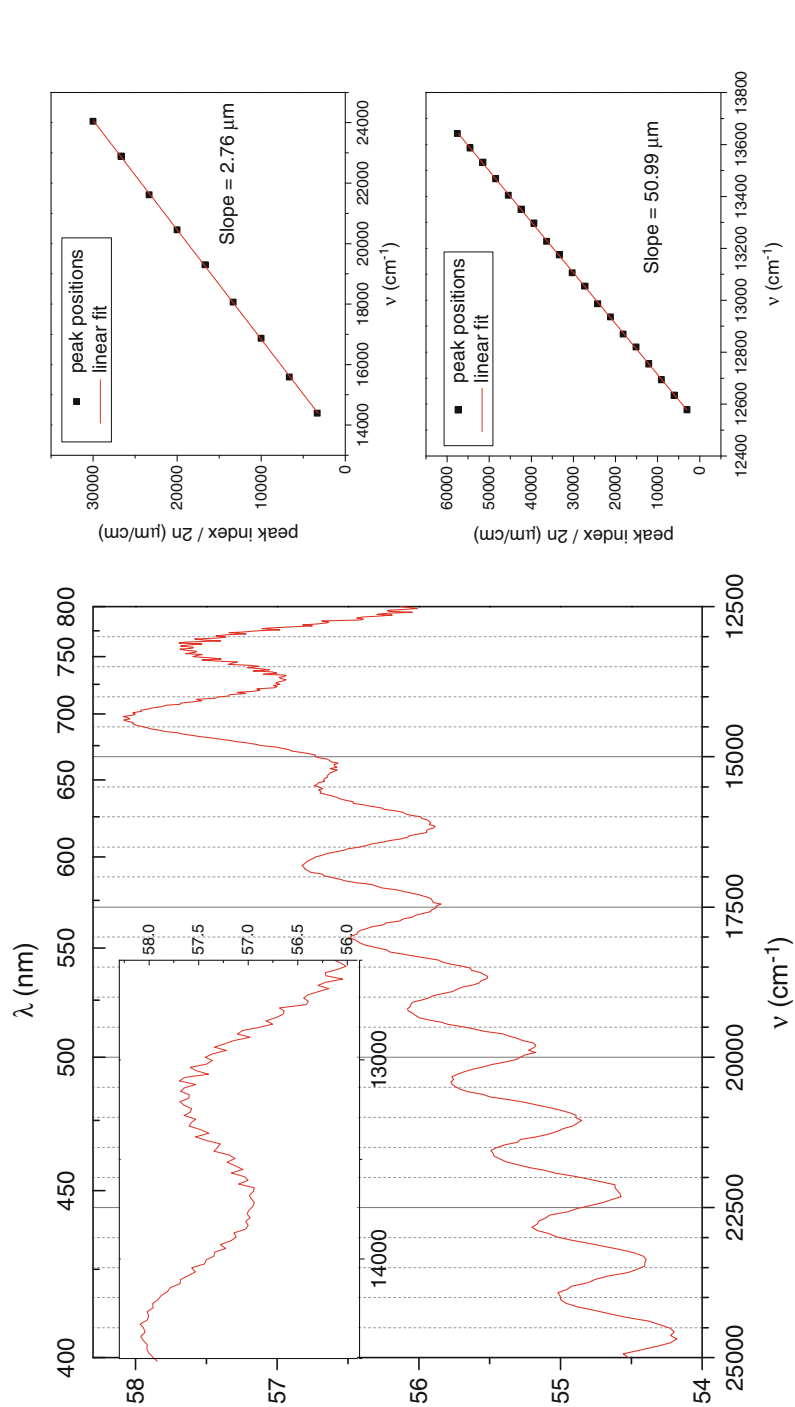

Fig. 2.7 Transmission spectrum of a two film system at normal incidence. The system consists of a polyester film on a thick polyester substrate with a thin adhesive layer between the two. The refraction index of polyester was considered constant in the measured interval, for simplicity. The *inset* shows the portion of the spectrum at longer wavelengths in more detail to resolve the higher frequency fringes. The graphics on the *right* show a plot of the fringes position against m/2n, where m is the fringe index number and n the index of refraction for the respective film. The slope of the line gives the thickness of the film directly. For index of refraction determination, we could measure at different angles of incidence, if the thickness is unknown, or plot the fringes position against m/2d if d is known

have several clear interference fringes. To improve the accuracy of the method is better to use a large number of well-defined fringes, that are not distorted by absorption bands of the films or substrate. A more general analysis of this method can be seen in reference [19].

2.3.8 Strengths and Limitations

The main strength of the spectrophotometry is the simplicity of the technique, requiring almost no sample preparation. It is a non-destructive technique, very flexible in terms of types of samples that can be measured. Its data interpretation and analysis is rather simple, and instrumentation is not very expensive.

Main limitations are that for some of the modalities a standard reference sample is needed. Another limitation is that proper calibration and alignment of the system is needed to generate accurate results. For most commercial instruments, however, this calibration is done automatically and the alignment is easy to perform. In diffraction grating based instruments, like most spectrophotometers, to sort out the higher order diffractions, it is necessary to use filters, which may lead to certain discontinuities on the spectrum.

2.4 Fourier Transform Infra-Red Spectroscopy (FTIR)

While diffraction grating based spectrophotometers are a powerful tool to collect transmission and reflection spectra in the UV to near infra-red range of the spectrum, they are not the best choice for measurements in the mid and far infra-red range. For measurements in the IR, dispersive instruments are not as efficient or convenient as the Fourier transform (FT) spectrometers. Generally, FT instruments have a higher throughput, better accuracy and precision, compared to grating based instruments.

The photons with energies in the infra-red range of the spectrum interact mostly with phonons and molecular vibrations and rotations, which depend strongly on the material's atomic structure. Thus, FTIR is a useful technique to probe the structural properties of matter.

A certain vibration mode needs to create a change on the dipole moment of the material to be active for absorption (IR active), i.e. to produce an absorption peak on that material's spectrum. This leads to the fact that symmetric modes of vibration usually do not cause absorption. They may, however, be present on the Raman scattering spectrum of the material. For that modality of spectroscopy, modes that cause a polarizability change are active. For that reason Raman is considered a characterization technique complementary to IR spectroscopy.

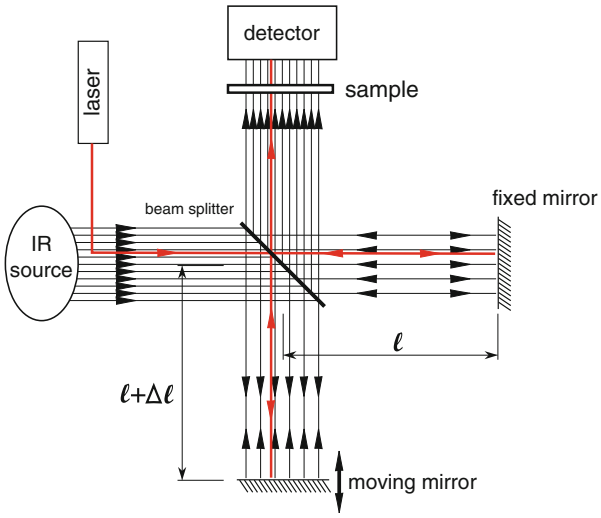

Fig. 2.8 The Fourier transform spectrometer is based on a Michelson interferometer with a moving mirror. The signal on the detector will be a composition of many superimposed frequencies, each the result of the interference of a different wavelength

2.4.1 Instrumentation

The FT spectrometer design is based on light interference rather than diffraction. Instead of using diffractive optics to separate spatially the wavelength components of the light, the FT spectrometer uses a Michelson interferometer with a movable mirror moving at a fixed frequency, and directs all wavelengths at once to the detector. The frequency of this mirror's movement is constantly monitored and calibrated using a reference laser, which grants the FTIR its greater precision and accuracy. This laser serves also as a real-time wavelength reference which is acquired simultaneously to data collection.

Its principle of operation lies on the interference between the light traveling through the two different arms of the interferometer as shown in Fig. 2.8. For a monochromatic light beam, when the path difference ($\Delta\ell$) between the two arms of the interferometer is an integer multiple of the wavelength, the beams will interfere constructively and when it is an integer multiple plus half of the wavelength they will interfere destructively and cancel each other. This will generate an oscillatory signal on the detector as a function of time. Different wavelengths interfere differently for given positions of the movable mirror. When monochromatic light passes through the interferometer, it creates an oscillating response on the detector. With polychromatic light, the presence of multiple wavelengths results in a superimposed signal oscillating in time with different frequencies (see Fig. 2.9). This combined signal is what we call an interferogram.

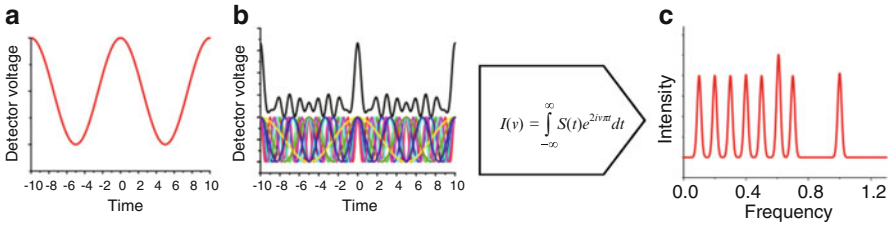

Fig. 2.9 A monochromatic light beam passing through the Fourier transform spectrometer creates an oscillating response on the detector (**a**). The signal from polychromatic light creates an interferogram (**b**), which can be deconvoluted by a Fourier transform to recover the frequency domain spectrum. The frequencies forming the interferogram will be represented by peaks whose amplitude is proportional to the intensity of the the light of that frequency impinging on the detector (**c**)

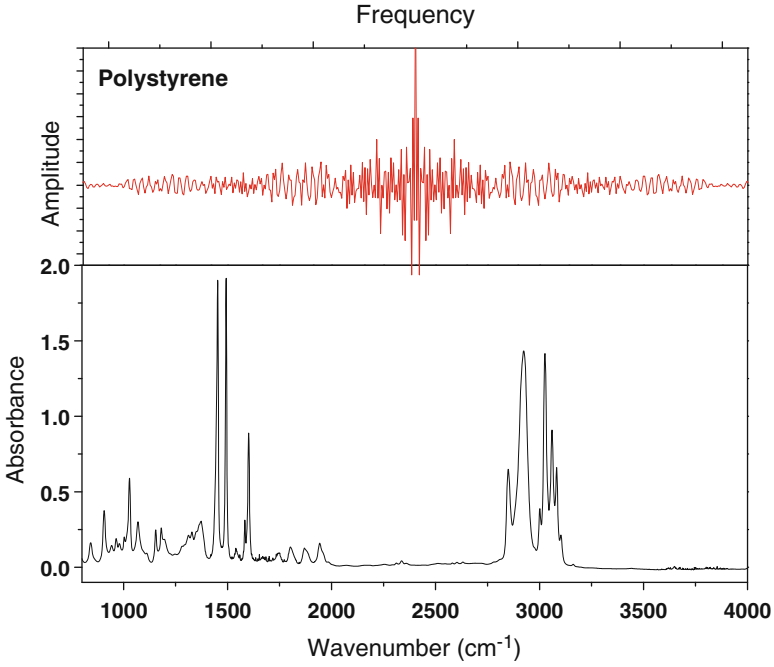

Fig. 2.10 Interferogram and corresponding FTIR spectrum for Polystyrene

To recover the frequency domain spectrum we apply a Fourier transform to the interferogram. The artificial example in Fig. 2.9 is formed with only eight different wavelengths. Figure 2.10 shows a real interferogram, and the corresponding experimental spectrum for polystyrene.

Since signal from all wavelengths is being acquired simultaneously for each period of the movement of the moving mirror, instead of scanning the light coming

from a diffraction grating through a slit, a much faster data collection is possible. The mirrors used on the interferometer have much less loss than a diffraction grating, so a higher throughput is also achieved using this approach. The simpler moving parts of the instrument and the use of a fixed wavelength laser for monitoring and calibrating the FTIR spectrometer mirror's movement grants the technique accuracy and precision that cannot be easily achieved with dispersion optics based spectrometers. The fact that the optics do not change during the experiment (no changing filters or gratings for different wavelengths) means that the FTIR spectra do not have the discontinuities that arise from those changes.

2.4.2 Transmittance

As with spectrophotometry, the most commonly used experiment performed with a FTIR spectrometer is measure the transmission of light through a sample as a function of wavelength. The basic theory behind the modality is the same as discussed in Sect. 2.3.2 above for the spectrophotometry, so instead of repeating it, here we will concentrate mostly on the differences. To compensate for the instrument and environment (usually air) contribution to the signal we collect a background spectrum, similarly to the baseline for the spectrophotometry, but no dark current spectrum is collected.

The raw spectrum obtained (T_0) is then divided by the background (B), to determine the contribution due solely to the sample, the absolute transmittance (T).

$$T = \frac{T_0}{B} \tag{2.18}$$

IR absorption is strong in most liquids and for measuring them, cells with very short path lengths are used.

2.4.2.1 KBr Pellets

For measuring IR transmission of powder samples, one of the most used techniques is the fabrication of pellets of a transparent material in powder form, mixed with a small amount of the powder to be measured. Usually 1–2 % of sample is more than enough to generate a good signal. The pellets are made by compressing the mixture with a suitable press, and mounted as any other solid film to be measured.

Several companies produce manual and hydraulic presses for the fabrication of FTIR pellets and a range of models are available with maximum loads from under 1 up to 40 t. The transparent powders used to mix with the sample, most often KBr, must be free of IR absorbing impurities, or those will introduce artifacts to the measured spectrum. These powders should be bought in FTIR or spectroscopy purity grade. These purity grades ensure that no IR absorbing impurities are present above a certain threshold. Some powders, even with greater purity, that are not spectroscopic

grade, may contain impurities that strongly absorb IR light, and will introduce peaks in the measured spectrum even in very small amounts. Besides KBr, other powders that are available for FTIR analysis are KCl, NaCl, CsI, and TiBr. Some are better than others depending on the desired range of the spectrum to be measured.

2.4.2.2 Nujol Method

Another popular method to measure powder samples is the Nujol method. Nujol is the trade name of an IR transparent non-volatile mineral oil, which is used to make a suspension of the powder to be measured. The suspension is then compressed between crystal plates (KBr or other suitable material) to be measured. Since Nujol exhibits strong absorption at 2,800–3,000, 1,450–1,465, 1,370–1,380, and 700–730 cm^{-1}, if the sample has peaks in these regions, another liquid that has no absorption in those spectral regions must be used to measure the absorption of the sample there. This method is particularly useful if the sample strongly absorbs moisture, since it helps to keep the sample dry.

2.4.2.3 IR Sample Cards

Polymer IR sample cards are available as an inexpensive disposable sample substrate for qualitative analysis of liquids or solutions. These usually consist of a polymer or crystal film held by a cardboard frame that can be mounted for transmission measurement. The most used polymers are PTFE and Polyethylene, due to their relatively flat IR spectra. PTFE has absorption peaks at 1,100–1,300 and 400–750 cm^{-1}, while Polyethylene at 2,800–3,000 and 1,400–1,500 cm^{-1}. Some companies also offer these cards with crystal films of NaCl, KBr, and KCl.

2.4.2.4 Data Acquisition Strategies

As discussed in Sect. 2.3.2.1, if we are measuring pure liquids and want to compensate for the transmittance of the container, we should not use the empty container to measure the background.

An important difference between measuring the spectrum in the UV-visible and in the infrared range is that in the latter, the water vapor and CO_2 present in air have strong absorption bands. Thus, it is useful to eliminate those molecules from the measurement environment. The majority of the FTIR instruments can have the sample chamber purged with dry N_2 or similar IR transparent atmosphere. It is important to verify that the level of these impurities is the same during the acquisition of the background and the data collection, otherwise artifacts from the difference in those levels will be present in the final spectrum.

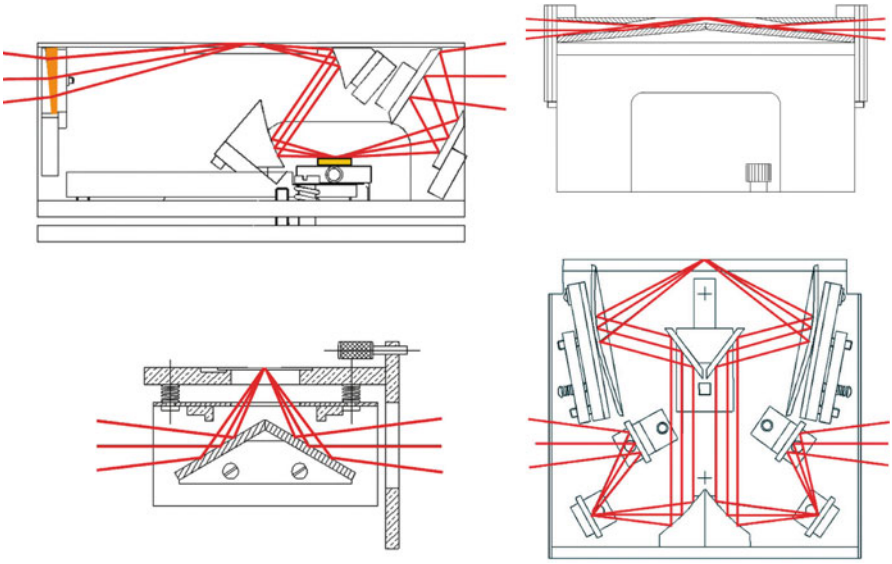

Fig. 2.11 Schematic representation of the beam paths of some popular FTIR specular reflectance accessories

2.4.3 Specular Reflectance

As with spectrophotometry, there are various accessories to the FTIR to allow for different experiments. Schematic representations of some of these accessories to measure specular reflectance are shown in Fig. 2.11. This modality of FTIR experiments are useful to measure thin films on reflective flat substrates, and bulk flat reflective materials. For very thin films shallower angles are recommended, as the optical path through the film will be longer.

2.4.4 Diffuse Reflectance

As is the case for spectrophotometry, several accessories for collecting diffuse reflectance based on integrating spheres or specially designed curved mirrors are available. The internal coating of integrating spheres designed to work in the near and mid-infrared is gold, which makes the sphere usable between 0.7 and 40 μm. The surface is made rough to ensure a strictly diffuse reflectance. The absorbance can be calculated from the diffuse reflectance using the Kubelka-Munk formula (Sect. 2.3.4). This modality of measurement is often called DRIFTS (Diffuse Reflection Infrared Fourier Transform Spectroscopy).

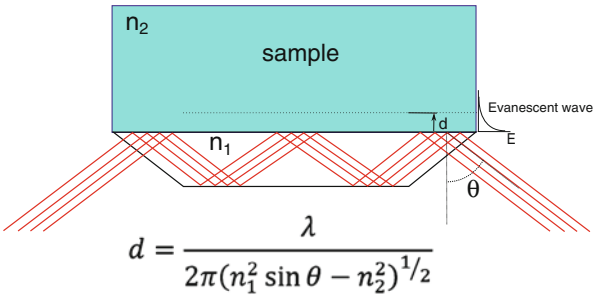

Fig. 2.12 Schematic diagram of an ATR prism. d denotes the evanescent wave penetration depth into the sample. n_1 and n_2 are the indexes of refraction of the prism and sample, respectively. λ is the light wavelength and θ its the angle of incidence

2.4.4.1 Data Acquisition Strategies

Filling the sample cup for DRIFTS of powder samples properly is important, since different filling procedures may alter the material packing or distribution and lead to different results. The proper way to fill the cup is to overfill it, then remove the excess with a spatula or razor blade, so the cup is filled to the brim and the powder surface level. Do not tap the cup, as this makes the smaller particles to sink and larger particles to surface, possibly changing the reflected light intensity.

2.4.5 ATR

Another method used to collect absorption spectra from samples in the infrared range of the spectrum is called attenuated total reflection (ATR). Its principle is based on the frustration of the total internal reflection in a prism that is in contact with the sample being measured. Total internal reflection happens when light traveling in a high refractive index material impinges on the interface to a lower refraction index at an angle greater than the critical angle. If we consider light traveling between two different media, when it crosses the interface between the media it changes its speed and is deflected at an angle related to the angle of incidence according to Snell's law:

$$n_1 \sin\theta_1 = n_2 \sin\theta_2, \tag{2.19}$$

where, n_1 and n_2 are the indexes of refraction of the two media and θ_1 and θ_2 are the angles of incidence and refraction. If $n_1 > n_2$, for a critical angle of incidence $\theta_c = \arcsin\frac{n_2}{n_1}$, $\theta_2 = \frac{\pi}{2}$ and the light will reflect completely and not cross the interface. The electric field of the light in the medium two decays exponentially as shown in Fig. 2.12. If within the decay distance d the light is absorbed, this will frustrate the total reflection. This is the principle of the ATR method.

Common materials for ATR prisms are ZnSe, diamond, Ge, and Si. The choice of crystal will depend on the spectral range, chemical compatibility with the sample, and pressure between sample and prism to be used for the measurements.

There are several different configurations for commercially available ATR accessories. The type of sample, its physical properties and state are important factors to be taken into account when selecting the proper system. The sample must make very good contact with the ATR crystal to obtain a good spectrum. Typical penetration depths are of the order of 0.5–2 μm. Liquid samples are usually easier to measure than solid samples due to the better contact with the prism. With solid samples it is common to use clamping systems that force the sample against the ATR crystal for better contact. Many factors on sample preparation, like homogeneity of the sample, pressure used [20], type of ATR system, crystal material, can affect the final spectrum and must be taken into account when comparing spectra between different samples and systems.

2.4.6 Applications

Perhaps the best known application of IR spectroscopy is identification of chemical compounds in a diversity of samples, as food products, drugs, forensic samples, etc. None the less, IR spectroscopy has a wide range of applications beyond that, which include, among many others:

- Determination of concentration of chemical components (quantitative analysis).
- Determination and observation of reaction kinetics, phase transition, and process evolution.
- Structural characterization of materials.
- Atmospheric studies (trace gases, analysis of fires and smoke, automotive emission analysis, etc.)
- Criminal forensic analysis.
- Vibrational spectroscopy of materials.
- Explosive and controlled substances detection and identification.
- Non-invasive clinical diagnosis.
- Food and drug analysis.

Table 2.3 gives a list of a few general uses of IR spectroscopy on the characterization of different types of materials, listing the most commonly used accessories for that application, and a few observations about the measurement procedure.

2.4.6.1 Application Example: Material Identification by FTIR

One of the best known applications for the FTIR is the identification of unknown substances or confirmation of the presence of a substance in a given sample. The normal vibration modes of atoms in molecules and solids will depend strongly on

Table 2.3 Some common applications of IR spectroscopy with usual accessories needed for the specific application

Type of sample	Application	Accessories needed	Observations
Liquids and gases (pure)	IR transmission and absorption spectra, vibrational and rotational modes	Transmission	Due to strong absorption in the IR by most liquids, cells with short path lengths are typically used for those samples
	Chemical identification		From comparison with spectra libraries
	Trace detection		From presence of characteristic absorption peaks on IR spectrum
Liquids and gases (mixtures and solutions)	IR transmission and absorption spectra, vibrational and rotational modes	Transmission	Baseline with solvent must be collected
	Concentration of components		From quantitative analysis
	Chemical composition		From comparison with spectra libraries
	Reaction kinetics, process monitoring		May require special flow cells
	Trace detection		From presence of characteristic absorption peaks on IR spectrum
Liquids	IR absorption spectra	ATR	
Solid (powders)	Diffuse IR reflectance and absorption spectra	DRA with powder samples holder	For strongly absorbing powders, dilution with KBr or other non IR-absorbing powders is recommended
	IR transmission and absorption spectra, vibrational, phonon, and rotational modes	Crystal pellet press. Transmission	
	IR absorption spectra	ATR	Careful sample preparation is advised. Only a few microns of the sample is measured, which raises difficulties for inhomogeneous samples

(continued)

Table 2.3 (continued)

Type of sample	Application	Accessories needed	Observations
Solid (bulk)	IR transmission and absorption spectra	Transmission	
	Specular reflectance spectra	SRA	
	Diffuse reflectance spectra	DRA	
	Diffuse transmission spectra		
	Thickness	All	From interference fringes for semitransparent or transparent samples, with two parallel and flat surfaces
	Vibrational, phonon, and rotational modes		From IR absorption peaks
	Chemical composition		From comparison with spectra libraries
	Concentration of components		From quantitative analysis
Solid (thin film on substrate)	Transmittance spectra	Transmission	Requires transparent substrate
	Specular reflectance spectra	SRA	
	Diffuse reflectance spectra	DRA	
	Diffuse transmission spectra		Requires transparent substrate
	Vibrational, phonon, and rotational modes	All (type of substrate may limit which accessory may be used)	From IR absorption peaks
	Thickness		From interference fringes for semitransparent or transparent films, with two parallel and flat surfaces
	Chemical composition		From comparison with spectra libraries
	Concentration of components		From quantitative analysis

This table does not intend to be exhaustive of all uses of IR spectroscopy and FTIR. Its objective is to give a few examples of common applications of that spectroscopy modality for each type of sample

its bounds to its first neighbors, but also be affected by their second and even more distant neighbors, although less strongly. This makes the IR spectra from a substance rather unique, serving as a fingerprint of that substance. The more distinct bounds are present in the molecule, the more distinct vibration modes are possible. This makes these spectra quite rich for more complex molecules, with many allowed vibration modes.

The usual procedure for using FTIR and other IR spectroscopy modalities for substance identification is to compare the experimental spectrum to an existing spectral database, which contains the spectrum of many different known substances. If a match is found in the database, the substance is the same as the one which was used to obtain the database spectrum. Constructing an accurate database is time consuming and requires extreme care on the measurement of the spectrum from pure substances, to avoid artifacts and extraneous vibration modes due to impurities or sample degradation. For this reason, commercially available databases are usually quite expensive. These databases often come with software capable to search it for a match of the experimental spectrum, some being able to combine a few spectra in the database, for the cases when the experimental spectrum comes from a mixture of different substances. When this is the case, prior knowledge of most of the mixture components and analysis with complementary characterization techniques is highly recommended, to avoid false matches. On the example shown in Fig. 2.13 our experimental spectrum is shown together with the best matches encountered in the database. From direct comparison we can verify that our substance is polypropylene. The presence of a few evenly spaced peaks can be noticed on the experimental spectrum of our unknown polymer. Those are interference fringes and could be used to find the thickness of our film. When these fringes are too prominent, they may interfere on the ability for the software to find a good match. One easy way to minimize the intensity of these fringes is to measure at an angle of incidence close to the Brewster angle (see pages 348–350 from reference [2]) for the material. In practice, if one doesn't know the Brewster angle he can change the angle of incidence while observing the spectrum, to find the angle for which the fringes will be the weakest.

It is not always possible to obtain a good match for our experimental spectrum. The most common causes are impurities present in our sample, spectral artifacts, and use of a database that doesn't contain our substance. When using IR spectroscopy for identification of substances, always make sure that the match obtained makes sense. For example, if you obtain a match for your spectrum taken from a solid sample and the database spectrum was taken from a substance that is gaseous or liquid, you most likely have a false match. In these cases, if you look closely, you will find that several peaks on both spectra are not exactly matched or are not on both spectra.

2.4.7 Strengths and Limitations

Similarly to spectrophotometry, IR spectroscopy experiments are easy to perform, comparatively to other characterization techniques. The technique is mostly non-destructive, little sample preparation is required, and its analysis is relatively simple. There is a large body of research and reference materials for FTIR and many electronic libraries with thousands of spectra, allowing the use of automated

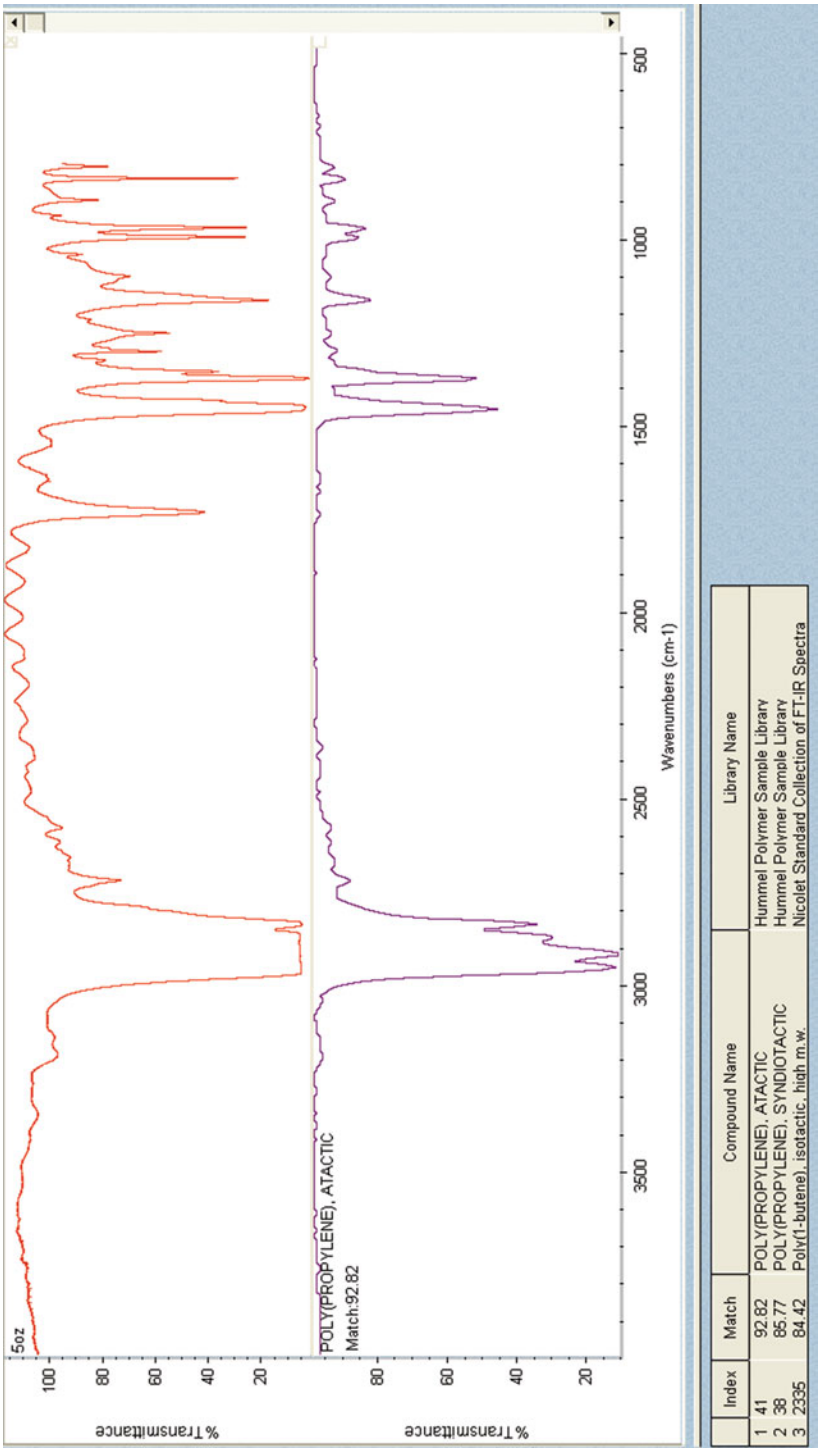

Fig. 2.13 FTIR spectrum of an unknown polymer and its match in the spectral library of the FTIR analysis software. From the close match we can identify our polymer as polypropylene

procedures and routines, which facilitate the use of FTIR for chemical identification. The strong absorption that most materials exhibit in the IR grants the FTIR an extremely high sensitivity for trace amounts of sample.

On the down side, quantitative analysis is usually demanding. The strong IR absorption of some liquids, like water, makes them unsuitable as solvents for FTIR analysis.

2.5 Ellipsometry

Besides intensity and energy, another characteristic of light that can be affected when light interacts with matter and can, thus, be used on the characterization of materials is its polarization. The best known technique that uses the polarization of light to characterize materials is the ellipsometry. In ellipsometry we measure the change on the state of polarization of light upon reflection by or transmission through a sample, which depends on its complex dielectric function.

The complex dielectric function of a material defines how that material responds to an electromagnetic field and can be related to its electronic structure, optical properties, and conductivity.

Matrix representations are commonly used to provide a mathematical description of optical measurements in a compact and convenient manner. The Jones and the Mueller matrix representations are often used to describe the change in polarization state of the light upon interaction with a sample. In these representations, Jones and Stokes vectors represent the different polarization states of light, and matrices are used to represent elements which change those states, as optical elements or the sample being analyzed. Figure 2.14 illustrates a simple ellipsometer and shows the Jones matrix representations for each component in a general case.

A complete description of these representations can be found in several text books [21–23], and is beyond the scope of this chapter.

In ellipsometry, the quantity measured is the ratio (ρ) between the complex reflection coefficients with polarization parallel ($\widetilde{R_p}$) and perpendicular ($\widetilde{R_s}$) to the plane formed by the incident and reflected light beams.

$$\rho = \frac{\widetilde{R_p}}{\widetilde{R_s}} = \frac{\left|\widetilde{R_p}\right|}{\left|\widetilde{R_s}\right|} e^{j\left(\delta_p - \delta_s\right)}, \tag{2.20}$$

with δ_p and δ_s being the phases of $\widetilde{R_p}$ and $\widetilde{R_s}$, respectively, and $j = \sqrt{-1}$. This ratio is usually written as

$$\rho = \tan \Psi e^{j\Delta}, \tag{2.21}$$

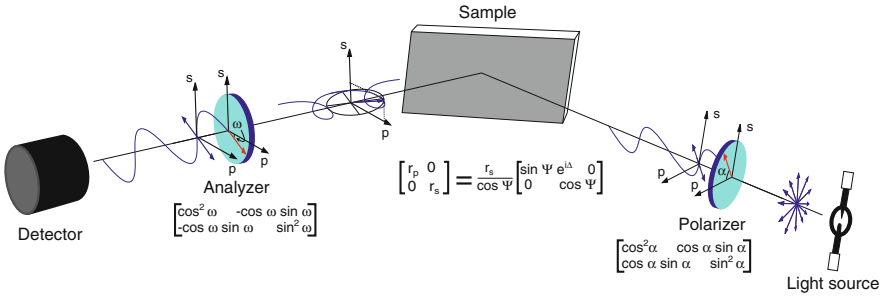

Fig. 2.14 Schematic diagram of a rotating analyzer ellipsometer (RAE) and the Jones matrix representation for each component. The *blue lines* represent the trajectory of the electric field vector of the propagating light. The difference in the representations of the analyzer and polarizer is due to the angles α and ω being measured in opposite directions

where Ψ and Δ are called ellipsometric angles. To obtain the optical properties of the material from the ellipsometric angles it is necessary to construct a physical model of the sample and fit the calculated values of Ψ and Δ from this model to the ones obtained experimentally.

2.5.1 Instrumentation

The ellipsometer is an instrument that consists of a light source delivering monochromatic light with a known polarization state, which is directed to the sample in a collimated beam, and a detector capable of detecting the polarization state of the light reflected by (or transmitted through) the sample.

Ellipsometry started in 1887 with Paul Drude, who developed the theory and performed the first ellipsometry measurements. Until 1975, ellipsometry wasn't a popular technique for materials characterization, since most ellipsometers were manually operated and data collection was very time consuming. With the development of fully automated spectroscopic ellipsometers in 1975, the technique became increasingly popular and the development of more efficient and complete ellipsometers accelerated drastically [24]. This rapid development of ellipsometry instrumentation allowed the range of applications of ellipsometry to grow significantly and the technique has become one of the most powerful optical characterization tools. Table 2.4 presents a brief chronology of this development until 1998. For a more complete description of the evolution and theory of operation of the various ellipsometer configurations, please see references [21–25]. Here we will present a very general description of some popular systems currently in use. Figure 2.15 shows a few of the possible configurations for ellipsometers.

Table 2.4 Chronology and other particulars of ellipsometry (E), spectroscopic ellipsometry (SE), and real-time spectroscopic ellipsometry (RTSE)

Year	Technique	Parameters determined	Number of data determined	Time taken (s)	Precision (°)	Author and reference
1887	E	Δ, Ψ	2	Theory and first experiment		Drude [26, 27]
1945	E	Δ, Ψ	2	3,600	$\Delta = 0.02$ $\Psi = 0.01$	Rothen [28]
1971	E	Δ, Ψ, R	3	3,600	$\Delta = 0.02$ $\Psi = 0.01$	Paik and Bockris [29]
1975	SE	Δ(λ), Ψ(λ)	200	3,600	$\Delta = 0.001$ $\Psi = 0.0005$	Aspnes and Studna [30]
1984	SE	Δ(λ), Ψ(λ)	80,000	3–600	$\Delta = 0.02$ $\Psi = 0.01$	Muller and Farmer [31]
1990	RTSE	Δ(λ, t), Ψ(λ, t)	2×10^5	0.8–600	$\Delta = 0.02$ $\Psi = 0.01$	Kim, Collins, Vedam [32]
1994	RTSE	Δ(λ, t), Ψ(λ, t), R (λ, t)	3×10^5	0.8–600	$\Delta = 0.007$ $\Psi = 0.003$	An, Collins et al. [33]

Adapted from reference [24], with permission

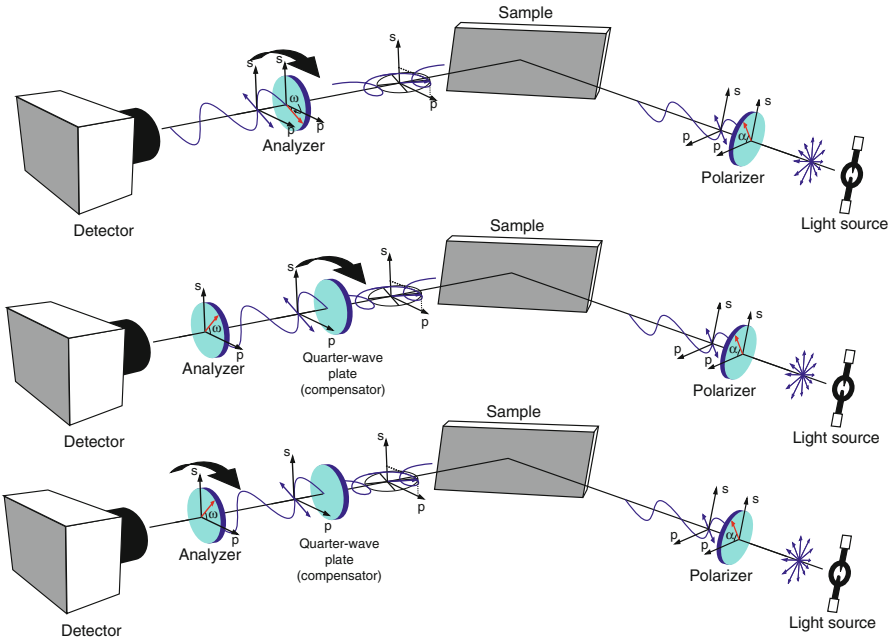

Fig. 2.15 Schematic diagram of a few possible configurations of automated ellipsometers. From the top to the bottom, a rotating analyzer ellipsometer (RAE), a rotating compensator ellipsometer (RCE), and a rotating analyzer with compensator ellipsometer (RACE)

2.5.1.1 The Null Ellipsometer

The null ellipsometer was the primary instrument used from the early days of ellipsometry until the mid 1970s to collect ellipsometric data. It was composed of a monochromatic light source, a polarizer, a quarter-wave plate (the compensator), an analyzer, and a detector. The working concept is that the linearly polarized light emerging from the polarizer would reflect on the sample. This reflection would introduce an ellipticity to the polarization of the light and the quarter-wave plate would be used to cancel it. Finally, the analyzer would be used to determine the polarization direction of the, once again, linearly polarized light. The azimuthal angles of the three components would then be used to determine the sample's effect on the probing light polarization. This instrument gets its name from the fact that its optical elements would be adjusted (rotated) until the signal on the detector was extinguished (null). Since this nulling process was inherently slow, it was eventually replaced by the rotating analyzer ellipsometer (RAE).

2.5.1.2 The Photometric Ellipsometers

While with the null ellipsometers the intensity of the light wasn't of significance, in the case of photometric ellipsometers that is the quantity that will allow us to obtain the ellipsometric parameters, Ψ and Δ. The most basic photometric ellipsometer, the RAE, depicted schematically in Fig. 2.14, is composed of a monochromatic light source, a polarizer, a rotating analyzer, and a detector. The signal from the detector will be a sinusoid plus a DC offset, and Ψ and Δ can be extracted by a Fourier analysis of the signal [25, 34]. The RAE and the equivalent RPE (rotating polarizer ellipsometer) are relatively simple instruments, but have the drawback of being less accurate when the light entering the detector is nearly linearly polarized, and that Δ cannot be measured in its full range (0–360°), due to fact that we cannot distinguish the handedness of the polarization of the light entering the analyzer. To alleviate this drawback, a quarter-wave plate can be inserted between the polarizer and the sample, thus allowing for the accurate determination of Δ over the full 0–360° range.

Both systems the RPE and the RAE present potential problems if the light source presents a measurable residual polarization, or the detector presents strong polarization sensitivity. The source residual polarization will require a correction curve for different positions of the polarizer for the case of the RPE, while a strong polarization sensitivity by the detector, as is typical for photomultipliers, will introduce difficulties for the RAE.

Another configuration for ellipsometers to tackle the inherent problems presented by the RAE and RPE is the rotating compensator ellipsometer. In this configuration, both polarizing elements (the polarizer and the analyzer) are kept in a fixed position, eliminating the sensitivity of the system to a residual input or output polarization. Besides, with this configuration it is possible to directly measure depolarization effects of the sample. Due to difficulties in constructing a rotating

quarter-wave plate that has the same retardance over the full spectrum only relatively recently systems with this configuration have become commercially available.

2.5.2 Analysis

Ellipsometry has become a very powerful characterization technique, as it can help us determine the dielectric function of the material being investigated, but some careful analysis to the ellipsometric data is necessary to obtain useful physical properties of the sample. As mentioned, the ellipsometer measures the change of the polarization state of light which interacted with our sample which is usually expressed as the ellipsometric parameters Ψ and Δ. From these data, the usual methodology to obtain the sample's physical properties we are interested on, requires the construction of an optical model of our sample. With this model on hand, we then calculate Ψ and Δ and compare them to the experimentally obtained values. If the agreement between the two data sets is not good, the model is changed and the process repeated, thus fitting our model to the experimental data. The accuracy of the results obtained will strongly depend on how accurately this model represents our sample. Thus, the more we know about our sample, the better. Especially for more complex samples, if nothing or very little is known about it, it is nearly impossible to successfully characterize it using ellipsometry alone.

To construct an accurate optical model of a sample, knowledge of the optical constants and thickness for each of the layers in the sample is required. The problem is, if we are using ellipsometry, we probably are trying to determine one or more of those characteristics for one or more of the layers, thus the need to fit the model to the experimental data. If all but either the thickness or the optical constants of one of the layers is known accurately, then it is possible to calculate the unknown characteristic for that layer directly from the experimental data. If more characteristics are not known, the fit is necessary using the unknowns as fitting parameters. More importantly, it is critical to make sure that our fit is unique and physically reasonable. In real cases it is common to have one or more of the fitting parameters correlated, such that small changes on one can be compensated by changes on the other without changing the final calculated Ψ and Δ too much. This makes it difficult to find a unique fit.

The simplest case for ellipsometric data analysis is the case of an isotropic optically thick homogeneous bulk sample with a flat surface, i.e. a sample constituted by one single homogeneous material, which is thick enough so light can't reach the back surface of the sample. In this simple ideal case, no fit is necessary, and the optical constants can be directly calculated from the experimental ellipsometric parameters. Most opaque bulk samples will have a thin oxide overlayer, which will contribute significantly to the measured ellipsometric parameters, and render the direct calculation of optical constants for the bulk material from Ψ and Δ inaccurate. A very thorough review of several techniques for

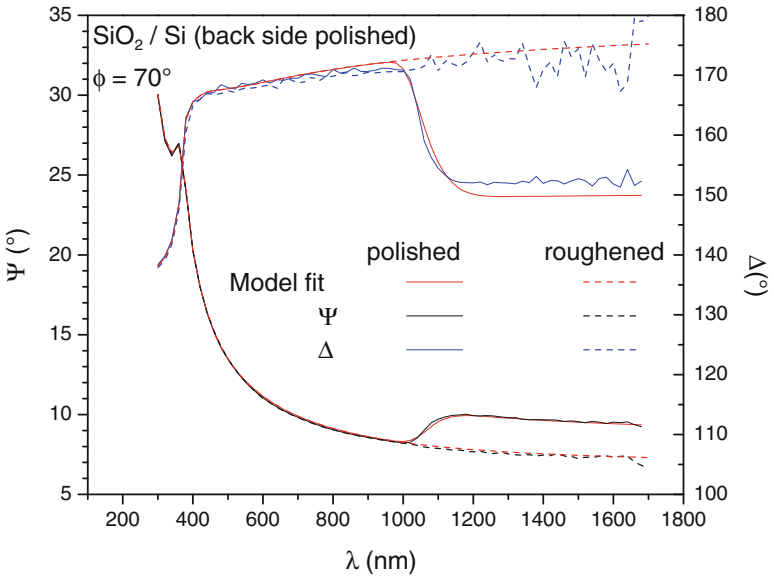

Fig. 2.16 Ellipsometric spectra for a sample of SiO_2 on a Si substrate with both sides polished, taken before (*solid lines*) and after (*dashed lines*) roughening of the back side. The model fit to the data taken before roughening the back side of the sample, include the effect of the reflection from the back side of the substrate. The fit to the data taken after roughening does not include that effect

obtaining the optical constants of bulk solids with surface overlayers is given in the Chap. 5 of reference [35].

In the case of bulk samples which are transparent, it is necessary to be careful with reflections from the back surface of the sample reaching the detector. For thick samples (typically 100 μm or thicker), this reflection will mix incoherently with the light reflected by the front surface of the sample, resulting in a partially polarized beam. There are basically three ways to deal with this problem (See Fig. 2.16):

- Eliminate the back surface reflection. This can be achieved by a number of ways, as roughening the back surface, so it doesn't reflect light specularly, coupling the sample back surface with a much thicker (or back surface roughened) piece of index matched material, painting the back surface with absorbing material (not always effective), etc. Figure 2.16 shows the effect of roughening the back surface to eliminate its contribution to the reflected signal.
- Spatially filter the reflection from the back surface from entering the detector-which is very effective, but not practical for not thick enough samples, when the front and back reflections overlap significantly.
- Include the effects of the back surface reflection in the model, which makes the analysis a little more complicated, but can be accomplished successfully if a good model is used. For a more detailed description, see Sect. 5.4.4 of reference [22]. The fit in Fig. 2.16 for the polished sample is done taking the reflection from the back surface of the substrate into account.

Table 2.5 Some optical constants model functions and applications

Model function	Mathematical expression [22, 25]	Applicability
Lorentz model	$\varepsilon = 1 + \frac{e^2 N_e}{\varepsilon_0 m_e} \frac{1}{(h\nu_0)^2 - (h\nu)^2 + i\Gamma h\nu}$	Metals, semiconductors (when $h\nu > h\nu_0$), conducting oxides
Sellmeier model	$\varepsilon_1 = 1 + \frac{e^2 N_e}{\varepsilon_0 m_e (2\pi c)^2} \frac{\lambda_0^2 \lambda^2}{\lambda^2 - \lambda_0^2}, \varepsilon_2 = 0$	Transparent dielectrics and semiconductors (when $h\nu < h\nu_0$)
Cauchy model	$n(\lambda) = A + \frac{B}{\lambda^2} + \frac{C}{\lambda^4} + \ldots, k = 0$	Transparent dielectrics and semiconductors (when $h\nu < h\nu_0$). Note: to model an absorbing dielectric, the extinction coefficient can take the form $k(\lambda) = \alpha e^{\beta\left(\frac{1}{\lambda} - \frac{1}{\lambda_0}\right)}$ [34]
Tauc-Lorentz model	See reference [36]	Amorphous materials, transparent conducting oxides
Drude model	$\varepsilon = \varepsilon_\infty \left(1 - \frac{h^2 e^2 N_f}{4\pi^2 \varepsilon_0 \varepsilon_\infty m^* \left((h\nu)^2 - i\Gamma h\nu\right)}\right)$	Free electrons and free carriers absorption

For layered samples, the thickness and optical constants of a particular layer will always be correlated parameters. That means that it is not possible to accurately determine both, the thickness and optical constants for a given layer, with just one ellipsometric spectrum. To be able to resolve this correlation it is necessary to collect data for a set of samples with different thicknesses for the layer in question and identical otherwise. Then, by fitting the set of ellipsometric spectra generated, the correlation between the two parameters can be reduced.

Another very useful technique when performing data analysis is the parameterization of the optical constants, i.e. using mathematical functions to describe the wavelength dependency of those optical constants. This technique drastically reduces the number of fitting parameters. It can also help reducing the strong parameter correlations that occur when fitting the optical constants at each wavelength independently. There are many different model functions that can be applied to each different material system. For a more complete theory and applicability of these model functions refer to the excellent books by Fujiwara [22] and Tomkins and Irene [25]. The best ellipsometry software packages in the market fully support this analysis, with many of the model functions already pre-programmed and with the capability for programing custom functions as well. Table 2.5 gives a brief overview of a few model functions and their applicability.

The effective medium approximation can be used to model the effect of structured surface and interfaces, such as surface roughness and imperfect interfaces on the ellipsometric data. Furthermore, alloying, graded composition, and volume fractions in composite materials can also be modeled using this approximation [22]. To be valid, however, the sizes of the domains need to be considerably greater than atomic dimensions and smaller than $\lambda/10$. Additionally, the optical constants of the materials in question cannot depend on the shape and size of the domain.

2.5.3 Data Acquisition Strategies

The more layers we want to characterize at once, the harder it is to have all parameters uncorrelated, which in turn will reduce the accuracy of the results. There are a few tips, though that may help on the characterization of a more complex sample. If the sample has many layers, a popular method is to characterize it layer by layer. To do that it is necessary to grow as many samples as there are layers, with the first sample being the bare substrate, the second, the substrate plus the first layer, and so on until the last sample, which will be the complete sample. Proceeding in this manner, when we analyze the samples, we can use the data obtained on the analysis of each preceding sample as known parameters in the analysis of the next one.

Another important fact to remember when collecting spectroscopic ellipsometry data is that different ellipsometers have poor precision for some ranges of Ψ and Δ [25]. For example, the precision on Δ close to 0 or to 180 is poor for simple RAE, so it is useful to select the angles of incidence for our experiments in a manner to have Δ far from those angles for any given wavelength in at least one spectrum when using those instruments.

2.5.4 Applications

Applications for ellipsometry range from the simple determination of thin films thicknesses or optical constants, monitoring reactions and film growth [37], study of plasmonic effects in meta-materials [38], to structural and optical analysis of bio- and nano-materials [39, 40].

Some of the most typical applications include:

- Determination of optical properties of bulk materials.
- Determination of optical properties of thin films and layered materials.
- Determination of optical properties of anisotropic films and materials.
- Determination of thin and ultra-thin film thicknesses.
- Monitoring of reaction kinetics and crystal growth evolution.
- Surface and interface structural characterization.
- Study of electronic structure, from the dielectric function.
- Industrial quality control of glass panels with or without optical coatings

Spectroscopic ellipsometry is not limited to those applications, however and many non-traditional applications have been reported in the last decade or so, including:

- Study of optical and structural properties of bio-materials.
- Chiral liquid crystals characterization

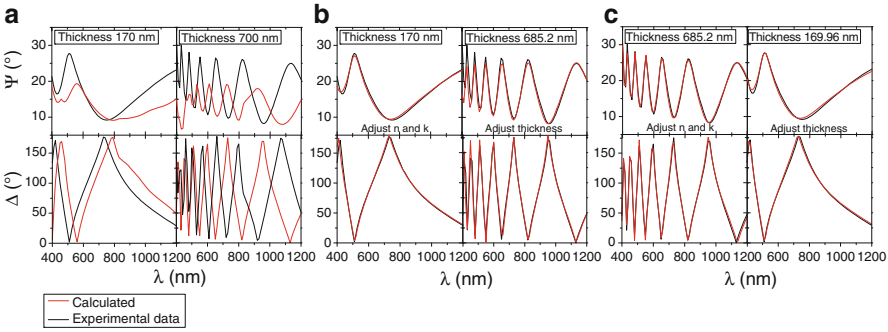

Fig. 2.17 Least squares fitting steps for two samples of TiO_2 on Si of nominal thicknesses 170 and 700 nm. Ellipsometric data was taken at the angle of incidence of 50°, 60° and 70°. Only the data for 70° is shown in the figure. Calculated spectra in (**a**), (**b**), and (**c**) show the results from initial parameters before fit, first round of fit, and second round of fit, respectively

- Design of specialty optical coatings
- Determination of free-carrier effective mass, mobility and concentration in doped semiconductors (for this application the use of magnetic fields and measurements in the far-infrared are required)

2.5.4.1 Application Example: Thickness and Optical Constants of a Thin TiO_2 Film on Si

One of the best known examples of the application of ellipsometry in materials characterization is the determination of the thickness of a thin transparent film. Here we will give an example of such application. We will use measurements at several angles of incidence from two samples with different thicknesses, to determine the films optical constants and their thickness. The method used here for obtaining those properties will be to fit the experimental data to physical models of the samples, using a least squares algorithm, which is the most widely used method on the commercially available packages. Barton and Urban have proposed another method which may render more accurate results. For details on their methodology see [41, 42]. Some ellipsometry software will allow for a more streamlined analysis of several samples than the one shown here, but the objective in this section is to provide the reader with a feeling on how to do this simple analysis with a more limited tool set.

The black lines in Fig. 2.17 show ellipsometric parameters measurements for two TiO_2 layers grown on Si wafers with a native oxide over layer. The calculated spectra shown in Fig. 2.17a were obtained by adopting a model with a top layer with nominal growth thickness and optical constants following the Cauchy relationship with wavelength (see Table 2.5) for modeling our top TiO_2 layer, a second layer of 2 nm native SiO_2 and an optically thick Si substrate. For this calculation, the optical constants for Si and SiO_2 were taken from [35] and the Cauchy parameters for

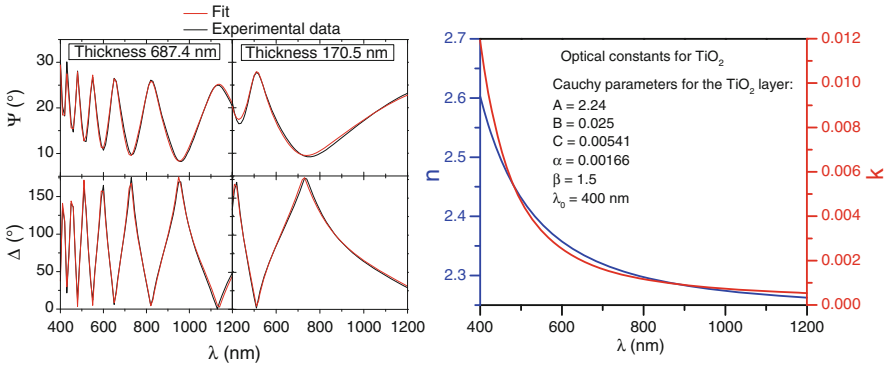

Fig. 2.18 Final results for the least squares fit of the proposed model to the experimental ellipsometric data obtained from samples of TiO_2 grown on Si with nominal thicknesses of 170 and 700 nm. Measurements were made at angles of incidence of 50°, 60°, and 70°. Only the data taken at 70° is shown here

modeling the initial TiO_2 were $A = 2.3$, $B = 0.01$, $C = 0$, and $\alpha = 0$. A least-squares algorithm was used to fit the calculated spectra to the experimental data by varying the optical constants of the thinner sample, then thickness for the thicker sample and the results are shown in Fig. 2.17b. Repeating the procedure, but swapping the samples, we got the results of Fig. 2.17c. The procedure is repeated a few times and the final results are shown in Fig. 2.18. In this example, we obtained reasonable dispersion curves for the optical constants of the two samples with very different thicknesses. Having several samples with different thicknesses when needing to obtain the optical constants and thickness of a layer is very useful, because it helps to reduce the correlation between those two fitting parameters. Whenever possible, confirmation of the data obtained in this manner with a complementary technique is always advisable.

2.5.5 Strengths and Limitations

One of the greatest strengths of ellipsometry is that it collects information about the change in phase (Δ), rendering the technique extremely sensitive to small changes in thickness and optical constants. That is the main reason it is widely applied on the measurement and monitoring of thin films growth and quality control in industry and basic research. Sub-angstrom variations in thin film thicknesses are easily detected using ellipsometry. For the same reason it is also ideal to study changes on surface and interface structure. The fact that ellipsometry detects the change of the polarization state of light by measuring a ratio of intensities makes the technique inherently more accurate than techniques which measure absolute intensities directly, as reflection or transmission. It is a non-contact technique that can be performed in-situ to monitor ultra-high vacuum

or hazardous environment processes. It is a non-destructive technique and applicable to a wide range of materials.

The main limitations of the technique are that being an optical characterization technique, it cannot be used to study interfaces buried in opaque materials, i.e. with no light access. It requires relatively flat surfaces and parallel interfaces with a non-zero specular reflectance to gather information about those interfaces. It is an indirect technique in the sense that it requires a physical model to be fitted to the experimental data to enable us to obtain physical properties of samples. Due to this fact it also requires some previous knowledge about the sample to avoid time-consuming analysis.

2.6 Raman Spectroscopy

In 1928 Sir Chandrasekhara Venkata Raman observed that, when illuminating a material sample with monochromatic light, in addition to the light scattered elastically (Rayleigh scattering), a small portion of the light was inelastically scattered, having its energy changed. The difference in energy of the emerging photons relative to the incident photons correspond to the energy that is absorbed or released by collective vibrations of the atoms in the sample, phonons in solids, normal vibration modes in molecules, liquids or gases. This scattering is known as the Raman effect; for its discovery and the development of the theory behind the effect, Sir Raman was awarded the 1930 Nobel Prize in Physics. Because the vibration levels of a sample are intrinsically dependent of its atomic structure, the Raman effect can be used as an effective tool for structural and chemical characterization, similarly to the IR spectroscopy. The Raman scattering is usually a very weak effect, typically with an intensity 3–5 orders of magnitude weaker than the Rayleigh scattering, which is itself, about 3–4 orders of magnitude less intense than the incident excitation light beam.

Raman scattered photons may present a higher or lower energy than the original incident photons, depending if it gains or loses energy to the vibration modes of the sample. Due to this fact, the Raman spectrum of a sample is composed typically by peaks symmetrically distributed around the central Rayleigh peak. The peaks with energy lower than the Rayleigh peak are termed Stokes peaks and anti-Stokes peaks is the term designating the peaks at a higher energy than the Rayleigh peak. Figure 2.3 shows the Raman spectrum for a PDMS sample where we can see the corresponding spectral features related to Stokes and anti-Stokes Raman scattering.

Raman and Rayleigh scattering can be understood as the light generated by oscillating electric dipoles in the material, induced by the incident excitation radiation. The induced dipole moment tensor μ' can be considered, in a first order approximation, a linear function of the applied field E:

$$\mu' = \alpha E \tag{2.22}$$

The α tensor is the polarizability of the material. Considering its modulation by the normal atomic vibrations of the material, for small amplitude oscillations near the equilibrium, the polarizability dependence on the normal coordinate Q associated with a normal mode of vibration can be written as:

$$\alpha = \alpha_0 + \left(\frac{\partial \alpha}{\partial Q}\right) Q = \alpha_0 + \alpha' Q \tag{2.23}$$

where α' is called the derived polarizability tensor. Treating the normal vibrations as harmonic:

$$Q = Q_0 \cos \omega t \tag{2.24}$$

and with the incident electric field being given by:

$$E = E_0 \cos \omega_0 t \tag{2.25}$$

the time dependence of the induced dielectric moment will be given by:

$$\mu' = \alpha_0 E_0 \cos \omega_0 t + \frac{1}{2} \alpha' Q_0 E_0 [\cos (\omega_0 - \omega) t + \cos (\omega_0 + \omega) t] \tag{2.26}$$

This means that the dipole will oscillate simultaneously with three frequencies, ω_0, $\omega_0 - \omega$ and $\omega_0 + \omega$. The first term of μ' describes the Rayleigh scattering while the second and third terms account for the anti-Stokes and Stokes Raman scattering corresponding to the normal mode of vibration Q. It can also be seen that while the Rayleigh scattering depends on the polarizability of the material at its equilibrium configuration, Raman scattering depends on the sensitivity of the polarizability to changes in the atomic configuration along the direction of the normal coordinates of vibration, reflected by α'. That means that if for a particular normal mode Q, $\alpha' = 0$, that mode of vibration is not Raman active. For IR absorption, a particular mode of vibration is active if the dipole moment changes with that vibration, i.e. when

$$\left(\frac{\partial \mu}{\partial Q}\right) Q \neq 0 \tag{2.27}$$

Since the Raman and IR activity are subject to different selection rules, as exposed above, the techniques are used as complementary characterization tools. For example, in the case of a homonuclear diatomic molecule, its stretching mode will be Raman active, but since there is no change of the dipole moment, it will be IR inactive, while a heteronuclear diatomic molecule will be both, Raman and IR active.

2.6.1 Instrumentation

As a versatile characterization tool, applicable on the analysis of gases, liquids and solids, and of a wide range of different materials including biological specimens, polymers, ceramics semiconductors, among many other, Raman spectroscopy instrumentation is available in a great variety of different setups, some more adapted to a specific application and some intended for a broader use. Commercial systems are available from portable, relatively inexpensive (for about US$15,000) models, to sophisticated tabletop confocal microscopic systems (some costing more than US $400,000). Since Raman scattering is a very low yield process, in the vast majority of the cases, the signal to noise ratio in a Raman measurement will be mainly limited by the number of Raman scattered photons reaching the detector. With that in view, when designing a Raman spectrometer, the light collection needs to be carefully optimized, by matching the correct acceptance angles from the sample all the way to the detector, and using high throughput collection optics and spectrometers.

Another important issue to take into account is the rejection of stray light and the Rayleigh scattering. Stray light can affect the spectrum in unpredictable ways, by reaching the detector through unforeseen paths, while Rayleigh scattered light may overwhelm the Raman signal at lower wavenumbers (closer to the Rayleigh line). To filter out those undesired contributions, the most common approaches are to use holographic or edge filters, or a double grating monochromator. Simpler instruments, or those instruments where the throughput is more important to the end goal, tend to use optical filters, while systems where spectral resolution and measurements of very small Raman shifts are needed, tend to use the double grating filtering scheme.

Raman peaks tend to be sharp and bunched close together, so spectral resolution is also an important factor to be taken into account when designing or acquiring a Raman spectrometer. Raman modes intensities and polarization properties are often dependent of the polarization state of the excitation source, sample orientation, temperature and crystallinity. For that reason, setups which allow for the selection of the polarization state of the excitation source, for sample conditioning and orientation and are capable of polarization selective detection, are common, as they enable a more complete characterization of the sample by Raman spectroscopy.

The typical setup is composed of an excitation laser source, which is directed to the sample to generate the scattering. The scattered light is collected by a lens or system of lenses, filtered to eliminate the Rayleigh scattered light, dispersed in photon energies, and directed to a detector.

2.6.2 Applications

Using Raman spectroscopy we are able to differentiate between various phases of a material with the same chemistry or regions of different chemical composition of a sample. It can be used to study the incorporation of impurities on a crystalline

matrix, to measure stress distribution in a sample, or monitor phase transitions, with temperature or pressure. For some materials, like graphene, it can even be used to determine the number of layers deposited. Used as a contrast mechanism in microscopy, it can be used to image regions of different chemistry or structure.

2.6.2.1 Application Example: Raman Spectroscopy of Carbon Incorporation in Cubic GaN

In this example, cubic-GaN samples doped with C concentrations from 2.7×10^{17} to 1.5×10^{19} cm^{-3} were grown by plasma-enhanced molecular beam epitaxy (MBE), in an effort to understand the incorporation of this p-type dopant in the lattice of c-GaN [43]. c-GaN is a metastable phase of this compound semiconductor, which is expected to have higher optical recombination efficiency then its hexagonal stable phase. That derives from the fact that in the hexagonal phase, spontaneous polarization caused by strain-induced piezoelectric fields result in a separation between electrons and holes. Since these fields do not occur in the cubic phase, a higher recombination of these carriers, followed by photoemission is expected. To obtain cubic GaN, samples were grown in Ga rich condition, which favors the growth of that phase, but also favors the formation of N vacancies and consequent break in lattice periodicity causing the appearance of the broad emission in the Raman spectrum of the sample with the lowest C concentration shown in Fig. 2.19a.

Another common defect in these samples are hexagonal inclusions, which manifest as a sharp peak at 568 cm^{-1} in that spectrum (Fig. 2.19b). As the C content of the samples increases, these peaks due to the defects of the GaN lattice and the broad emission start to decrease, indicating a decrease in the disorder in the samples. Moreover, the peaks corresponding to the crystalline cubic GaN become stronger with the addition of C dopants up to 4×10^{17} cm^{-3}, indicating an increased crystallinity. The presence of extraneous atoms into the lattice of a crystal leads, in general, to increased disorder and not the other way around. To understand what is happening in this case, we need to remember that the samples were grown on Ga-rich condition which favors the appearance of nitrogen vacancies, making them the dominant type of defect on these samples. The broad emission in the observed Raman spectra is believed to be largely caused by the break in periodicity from lattice distortions around these vacancies. Due to the similar atomic radii of N and C, if carbon atoms occupy the sites of these vacancies, the crystalline distortions disappear and the broad Raman emission is expected to quench as in the spectrum of the sample with a C concentration of 4×10^{17} cm^{-3}.

The incorporation of C into the GaN crystal lattice should give rise to a Raman mode characteristic of the localized vibration of the C atom in that lattice. For an impurity with a much smaller mass than either of the host atoms a vibration with a frequency in the forbidden region of the host lattice vibrations is expected. If, as in this case, the impurity atom has a mass similar to the host atom whose site it is occupying, the vibrational mode introduced by the impurity is in the range of the allowed modes of the perfect crystal. These modes are difficult to observe, unless

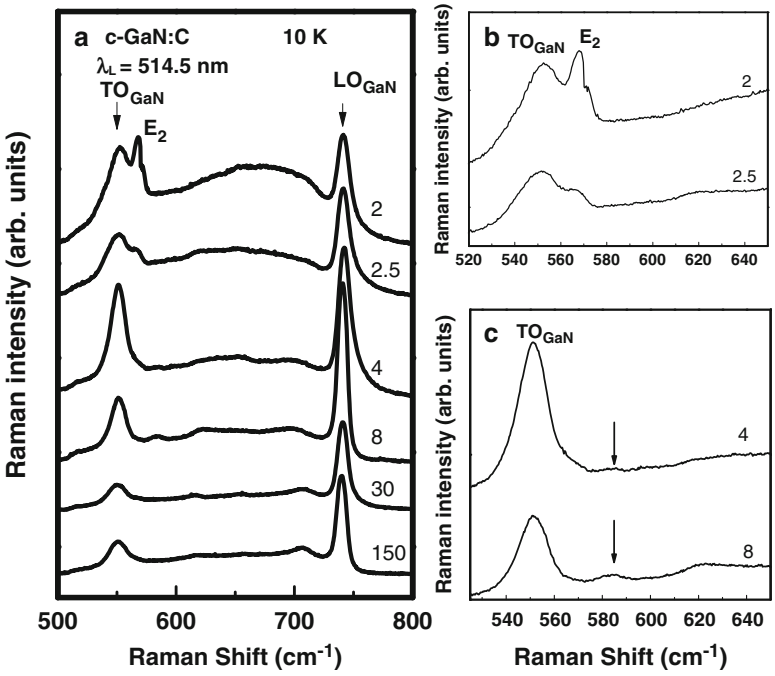

Fig. 2.19 (**a**) Raman spectra for a series of c-GaN doped with C. Dopant concentrations are noted over the right side of the curves in units of 10^{17} cm^{-3}. Panel (**b**) shows in greater detail the peak due to hexagonal phase GaN inclusions E_2, present on the samples with the lowest dopant concentrations. Panel (**c**) shows the peak attributed to substitutional C atoms on N sites

their frequency happens to lie at a point where the density of states of the vibrations of the pure crystal is small. A structure at 584 cm^{-1} that appears in the spectra from the two samples with the best crystalline quality (reproduced in Fig. 2.19c) is believed to be one of such modes. This assignment is supported by theoretical calculations using a valence force field model [43, 44]. This weak line starts to be visible for a C concentration of 4×10^{17} cm^{-3}, and gains strength as it increases up to the point where the C complexes begin to form. In the most doped samples, for which photoluminescence show strong C complex related emission, this line is completely quenched. This example demonstrates the use of Raman spectroscopy as an effective structural characterization tool.

2.6.3 Strengths and Limitations

Raman spectroscopy is one of the most versatile and powerful optical characterization techniques. It has applications which range from materials structural and chemical characterization [45] to medical diagnostics [46], to applications in the

fields of forensics and crime prevention [47], food sciences [48], biology [49], nanotechnology [50], geology [51], Industrial process and quality control [52], space exploration [53, 54], among many others. Its ability to investigate the vibrational spectrum of the samples constituting molecules makes it an ideal technique to complement IR spectroscopy. Its main limitation is that its intensity is very weak compared to the elastically scattered light and even to luminescence. That was one of the main reasons why the technique wasn't more widely used in the past. With the discovery of the laser and its rapid evolution, along with modalities of surface enhanced Raman scattering, resonance Raman, coherent anti-Stokes Raman scattering among others, this shortcoming is no longer a great limitation to the use of the technique.

2.7 Summary

Optical characterization of materials is a vast field of research that remains extremely active. Many new methodologies are developed each year that explore the interaction between photons of light and atoms to interrogate all kinds of atomic arrangements, from simple diatomic molecules to complex metamaterials. In general, optical techniques are non-destructive, relatively fast, and can be used to investigate innumerous materials properties, from electronic to chemical, to morphological.

Here, we hope we had offered a little flavor of this field in a few chosen examples, so the interested reader can gain an insight of the possibilities offered by optical characterization of materials. Many important techniques, as photoluminescence, the many varieties of optical microscopy, modulation spectroscopies, time-domain and transient optical spectroscopies, and many others were left out of this brief introduction as a compromise to remain adequately succinct to fit this book, yet give enough information about the few techniques mentioned, to be an useful reference.

References

1. SCHOTT optical glass data sheet-catalog. http://www.us.schott.com/advanced_optics/english/our_products/materials/data_tools/index.html
2. Hecht E (2002) Optics (fourth edition). Addison Wesley, San Francisco, CA
3. The NIST reference on constants, units, and uncertainty. http://physics.nist.gov/cuu/index.html
4. Weiner J, Ho P-T (2003) Light-matter interaction: fundamentals and applications, vol 1. Wiley, Hoboken, NJ
5. Szczytko J, Kappei L, Berney J, Morier-Genoud F, Portella-Oberli MT, Deveaud B (2005) Phys Rev B71:195313
6. Shay JL, Nahory RE (1969) Solid State Comm 7:945; Komkov OS, Glinskii GF, Pikhtin AN, Ramgolam YK (2009) Phys Status Solidi A 206:842
7. Moskovits M (1985) Rev Mod Phys 57:783

8. Merschjann C, Schoke B, Imlau M (2007) Phys Rev B76:085114
9. Lopez-Rios T (2012) Phys Rev B 85:125438
10. Tylley RJD (2011) Colour and the optical properties of materials: an exploration of the relationship between light, the optical properties of materials and colour. Wiley, West Sussex, England
11. Barybin A, Shapovalov V (2010) Int J Opt 2010:137572
12. Vargas WE, Castro D (2007) Appl Optics 46:502
13. Kubelka P, Munk F (1931) Z Techn Phys 12:593; Kubelka P (1948) J Opt Soc Am 38:448; Kubelka P (1954) J Opt Soc Am 44:330
14. Philips-Invernizzi B, Dupont D, Cazé C (2001) Opt Eng 40(6):1082
15. For more on the Kubelka-Munk theory and its applicability, see also: Yang L, Kruse B (2004) J Opt Soc Am A 21:1933; Yang L, Kruse B, Miklavcic SJ (2004) J Opt Soc Am A 21:1942; Yang L, Miklavcic SJ (2005) Opt Lett 30:792; Yang L, Miklavcic SJ (2005) J Opt Soc Am A 22:1866; Edström P (2007) J Opt Soc Am A 24:548; Kokhanovsky AA (2007) J Phys D Appl Phys 40:2210; Myrick ML, Simcock MN, Baranowski M, Brooke H, Morgan SL, McCutcheon JN (2011) Appl Spectroscopy Rev 46:140
16. Amirshahi SH, Pailthorpe MT (1994) Textil Res J 64:357
17. Lambert JH (1760) Photometria sive de mensura et gradibus luminis, colorum et umbrae. Eberhardt Klett, Augsburg, Germany; Beer A (1852) Bestimmung der Absorption des rothen Lichts in farbigen Flüssigkeiten. Annalen der Physik und Chemie 86:78
18. Finlayson AP, Tsaneva VN, Lyons L, Clark M, Glowacki BA (2006) Phys Stat Sol A 203:327
19. Harrick NJ (1971) Appl Opt 10:2344
20. Friedrich F, Weidler PG (2010) Appl Spectros 64:500
21. Azzam RMA, Bashara NM (1977) Ellipsometry and polarized light. North Holland Publ. Co., Amsterdam, The Netherlands
22. Fujiwara H (2007) Spectroscopic ellipsometry: principles and applications. Wiley, West Sussex, England
23. Schubert M (2004) Infrared ellipsometry on semiconductor layer structures: phonons, plasmons, and polaritons. In: Höhler G (ed) Springer tracts in modern physics, vol 209. Springer, Berlin, Germany
24. Vedam K (1998) Thin Solid Films 313–314:1
25. Tompkins HG, Irene EA (eds) (2005) Handbook of ellipsometry. William Andrew, Inc., Norwich, NY
26. Drude P (1887) Ann Phys 32:584
27. Drude P (1888) Ann Phys 34:489
28. Rothen A (1945) Rev Sci Instrum 16:26
29. Paik W, Bockris JO'M (1971) Surf Sci 28:61
30. Aspnes DE, Studna AA (1975) Appl Opt 14:220
31. Muller RH, Farmer JC (1984) Rev Sci Instrum 55:371
32. Kim YT, Collins RW, Vedam K (1990) Surf Sci 233:341
33. An I, Nguyen HV, Heyd AR, Collins RW (1994) Rev Sci Instrum 65:3489
34. Woollam JA (2010) Guide to using WVASE32®. J.A. Woollam Co., Inc., Lincoln, NE
35. Palik ED (ed) (1985) Handbook of optical constants of solids. Academic, San Diego, CA
36. Jellison GE Jr, Modine FA (1996) Appl Phys Lett 69:371; Erratum, Appl Phys Lett 69:2137 (1996)
37. Theeten JB (1980) Surf Sci 96:275
38. Oates TWH, Wormeester H, Arwin H (2011) Progr Surf Sci 86:328
39. Arwin H, Magnusson R, Landin J, Jarrendahl K (2012) Phil Mag 92:1583
40. Arwin H (2011) Thin Solid Films 519:2589
41. Barton D, Urban FK III (2007) Thin Solid Films 516:119
42. Barton D, Urban FK III (2011) Thin Solid Films 519:6284
43. Fernandez JRL, Cerdeira F, Meneses EA, Brasil MJSP, Soares JANT, Santos AM, Noriega OC, Leite JR, As DJ, Köhler U, Potthast S, Pacheco-Salazar DG (2003) Phys Rev B 68:155204

44. Santos AM, da Silva ECF, Noriega OC, Alves HWL, Alves JLA, Leite JR (2002) Phys Status Solidi B 232:182
45. Dutta B, Tanaka T, Banerjee A, Chowdhury J (2013) J Phys Chem A 117:4838
46. Feng S, Lin D, Lin J, Li B, Huang Z, Chen G, Zhang W, Wang L, Pan J, Chen R, Zeng H (2013) Analyst 138:3967
47. Tripathi A, Emmons ED, Guicheteau JA, Christesen SD, Wilcox PG, Emge DK, Fountain AW III (2010) Chemical, biological, radiological, nuclear, and explosives (CBRNE) sensing XI, 76650N. Proceedings of SPIE 7665, 27 April 2010. doi:10.1117/12.865769
48. Mohamadi Monavar H, Afseth NK, Lozano J, Alimardani R, Omid M, Wold JP (2013) Talanta 111:98
49. Bansal J, Singh I, Bhatnagar PK, Mathur PC (2013) J Biosci Bioeng 115:438
50. Chrimes AF, Khoshmanesh K, Stoddart PR, Mitchell A, Kalantar-zadeh K (2013) Chem Soc Rev 42:5880
51. Marshall CP, Marshall AO (2011) Spectrochim Acta Part A 80:133
52. Sarraguça MC, De Beer T, Vervaet C, Remon J-P, Lopes JA (2010) Talanta 83:130
53. Strazzulla G, Baratta GA, Spinella F (1995) Adv Space Res 15:385
54. Jaumann R, Hiesinger H, Anand M, Crawford IA, Wagner R, Sohl F, Jolliff BL, Scholten F, Knapmeyer M, Hoffmann H, Hussmann H, Grott M, Hempel S, Köhler U, Krohn K, Schmitz N, Carpenter J, Wieczorek M, Spohn T, Robinson MS, Oberst J (2012) Planet Space Sci 74:15

http://www.springer.com/978-1-4614-9280-1

Practical Materials Characterization
Sardela, M. (Ed.)
2014, VII, 237 p. 118 illus., 92 illus. in color., Hardcover
ISBN: 978-1-4614-9280-1